

# Ophicalcites from the northern Pyrenean belt: a field, petrographic and stable isotope study

Camille Clerc, Philippe Boulvais, Yves Lagabrielle, Michel De Saint Blanquat

# ► To cite this version:

Camille Clerc, Philippe Boulvais, Yves Lagabrielle, Michel De Saint Blanquat. Ophicalcites from the northern Pyrenean belt: a field, petrographic and stable isotope study. International Journal of Earth Sciences, Springer Verlag, 2014, 103 (21), pp.141-163. <10.1007/s00531-013-0927-z>. <i sub-00944405>

# HAL Id: insu-00944405 https://hal-insu.archives-ouvertes.fr/insu-00944405

Submitted on 10 Feb 2014  $\,$ 

**HAL** is a multi-disciplinary open access archive for the deposit and dissemination of scientific research documents, whether they are published or not. The documents may come from teaching and research institutions in France or abroad, or from public or private research centers.

L'archive ouverte pluridisciplinaire **HAL**, est destinée au dépôt et à la diffusion de documents scientifiques de niveau recherche, publiés ou non, émanant des établissements d'enseignement et de recherche français ou étrangers, des laboratoires publics ou privés.

1	Submitted to International Journal of Earth Sciences	Review 2
2		
3		
4	Ophicalcites from the Northern Pyrenean Belt: a field, petro	ographic and
5	stable isotope study.	
6		
7	by:	
8	Camille Clerc (1), Boulvais Philippe (2), Yves Lagabrielle (3) and Michel de	e Saint Blanquat
9	(4)	
10		
11	(1) Laboratoire de Géologie, CNRS-UMR 8538, Ecole Normale Superieure, 2	4 rue Lhomond,
12	75231 Paris Cedex 5, France.	
13	(2) Géosciences Rennes, CNRS-UMR 6118, Université de Rennes 1, Camp	us de Beaulieu,
14	35042, Rennes Cedex, France	
15	(3) Géosciences Montpellier, CNRS-UMR 5243, Université de Montpellier 2,	Place Eugène
16	Bataillon, 34095 Montpellier, France	
17	(4) GET, CNRS-UMR 5563, Université Paul Sabatier, 14 avenue Edouar	d Belin, 31400
18	Toulouse, France.	
19		
20	Corresponding author:	
21	Camille Clerc	
22	clerc@geologie.ens.fr	

23 Abstract

24

Brecciated and fractured peridotites with a carbonate matrix, referred to as 25 26 ophicalcites, are common features of mantle rocks exhumed in passive margins and midoceanic ridges. Ophicalcites have been found in close association with massive peridotites, 27 which form the numerous ultramafic bodies scattered along the North Pyrenean Zone (NPZ), 28 on the northern flank of the Pyrenean belt. We present the first field, textural and stable 29 isotope characterization of these rocks. Our observations show that Pyrenean ophicalcites 30 belong to three main types: (1) a wide variety of breccias composed of sorted or unsorted 31 millimeter-to meter-sized clasts of fresh or oxidized ultramafic material, in a fine-grained 32 calcitic matrix; (2) calcitic veins penetrating into fractured serpentine and fresh peridotite; and 33 34 (3) pervasive substitution of serpentine minerals by calcite. Stable isotope analyses (O, C) have been conducted on the carbonate matrix, veins and clasts of samples from 12 Pyrenean 35 ultramafic bodies. We show that the Pyrenean ophicalcites are the product of three distinct 36 genetic processes: i) pervasive ophicalcite resulting from relatively deep and hot hydrothermal 37 activity; ii) ophicalcites in veins resulting from tectonic fracturing and cooler hydrothermal 38 activity; and iii) polymictic breccias resulting from sedimentary processes occurring after the 39 exposure of subcontinental mantle as portions of the floor of basins which opened during the 40 mid-Cretaceous. We highlight a major difference between the Eastern and Western Pyrenean 41 ophicalcites belonging respectively to the sedimentary and to the hydrothermal types. Our 42 data set points to a possible origin of the sedimentary ophicalcites in continental endorheic 43 basins, but a post-depositional evolution by circulation of metamorphic fluids or an origin 44 45 from relatively warm marine waters cannot be ruled out. Finally, we discuss the significance of such discrepancy in the characterics of the NPZ ophicalcites in the frame of the variable 46 exhumation history of the peridotites all along the Pyrenean realm. 47

49

- 51 Key words: ophicalcite, ophicarbonate, stable isotopes, oxygen, carbon, veins, matrices,
- 52 Pyrenees, Lherz, Urdach, mantle exhumation, tectonic fracturation, hydrothermalism,
- 53 sedimentary deposits.

## 54 I. Introduction

During uplift and exhumation of the sub-continental mantle, the peridotites are commonly 55 serpentinized through interactions with fluids, with direct consequences on their bulk density 56 and their rheological, seismic, gravimetric and magnetic properties (Brun & Beslier 1996; 57 58 Boschi et al. 2006). In oceanic and passive margin environments, besides serpentinization, the peridotites show evidence of carbonation expressed through the occurrence of a bimodal, 59 ultramafic and carbonate association known as ophicalcites or ophicarbonates (Spooner & 60 Fyfe 1973; Bonatti et al. 1974; Dietrich et al. 1974; Gianelli & Principi 1977; Ohnenstetter 61 1979; Lemoine 1980; Cortesogno et al. 1981; Lagabrielle & Cannat 1990). More recently, the 62 carbonation of the exhumed mantle rocks has been clearly described as the last event affecting 63 faulted rocks uprising along oceanic detachment faults at the axis of slow-spreading ridges 64 (Picazo et al. 2012). 65

Ophicalcites were first discovered in the Ligurian Alps (Bonney 1879), and then described in 66 many ophiolite sequences (see Artemyev & Zaykov 2010 and Bogoch 1987 for a 67 comprehensive historical literature on ophicalcites). Ophicalcites commonly display large 68 variations in the proportions of ultramafic and carbonate material. They range from in-situ 69 fractured peridotites with carbonate infill, through clast-supported breccias with multiple 70 generations of carbonate infilling and internal sediments, to matrix-supported breccias. 71 Lemoine et al. (1987) distinguish two main types of ophicalcite. Ophicalcite type 1 (OC1) is 72 represented by massive serpentinites exhibiting a dense mesh of calcite-infilled fractures. 73 Ophicalcite type 2 (OC2) refers to sedimentary breccias having a calcitic matrix, often 74 75 deposited above ophicalcite of type 1. The clasts comprise sorted or unsorted millimeter- to meter-sized fresh or oxidized ultramafic fragments. In some cases, exotic clasts of gabbroic or 76 basaltic composition can be observed. The matrix of OC2 is either a fine-grained calcitic 77

sediment or a cement consisting of sparry calcite. It varies in color from red to pink and gray
to green, depending on the chlorite or hematite content; sparry calcite is generally white.
Ophicalcites often record a polyphase history, revealed by different generations of cements
and sediment infill, which can be highlighted by color changes, and bimodal grain distribution
(Abbate et al. 1970; Bonatti et al. 1974; Bernoulli & Weissert 1985; Lemoine et al. 1987;
Früh-Green et al. 1990).

Because of the wide variety of ophicalcites and their occurrence in different oceanic or 84 continental margin settings, it is important to recall that the term ophicalcite does not refer to 85 a genetic process, but to a generic rock-type. Among the processes invoked for their 86 formation one group refers to endogenic evolution, involving various deep seated phenomena 87 such as: (1) mantle originated gas seeps (Bonatti et al. 1974; Haggerty 1991; Kelemen et al. 88 2004); (2) magmatic intrusions (Cornelius 1912; Bailey & McCallien 1960); (3) contact and 89 regional metamorphism (Peters 1965; Trommsdorff et al. 1980) and (4) hydrothermal fluid 90 91 interactions (Cornelius 1912; Lavoie & Cousineau 1995; Artemyev & Zaykov 2010). Another group refers to surficial processes involving mechanical mixing of carbonates and ultramafic 92 rocks through tectonic crushing, sedimentary reworking and gravity-driven infilling of veins 93 and fractures (Bortolotti & Passerini 1970; Knipper 1978; Bernoulli & Weissert 1985; Früh-94 Green et al. 1990; Treves & Harper 1994; Treves et al. 1995; Knipper & Sharas'kin 1998). 95

In the French Pyrenees, ophicalcites have been reported in some ultramafic bodies associated with mid-Cretaceous basins and recently re-interpreted as resulting from mantle exhumation during Mid-Cretaceous rifting (Lagabrielle & Bodinier 2008; Lagabrielle et al. 2010; Jammes et al. 2009; Clerc et al. 2012). In order to document and to characterize the variable typology of ophicalcites and to decipher their origin with respect to exhumation processes, we have performed a comprehensive field, petrological and geochemical study of samples taken throughout the Pyrenees (fig. 1). We identify three types of ophicalcites related to three distinct genetic processes: i) pervasive ophicalcite resulting from replacement of ultramafic minerals due to relatively deep and hot hydrothermal activity, ii) ophicalcites as veins resulting from tectonic fracturing and cooler hydrothermal activity and iii) polymictic breccias resulting from syn-sedimentary processes. The first two types record the activity associated with the final emplacement of the peridotites, whereas the last one is associated with the final exhumation of mantle rocks as portions of the basement of newly formed basins.

109

# 110 II. Geological setting of the ultramafic Pyrenean bodies:

The Pyrenees are a narrow, 400 km long continental fold and thrust belt resulting from the 111 collision of the northern edge of the Iberian Plate and the southern edge of the European Plate 112 during the late Cretaceous to Tertiary (Choukroune & ECORS Team 1989; Muñoz 1992; 113 Deramond et al. 1993; Roure & Combes 1998; Teixell 1998). Triassic and Jurassic aborted 114 rifting events predated the development of a major Cretaceous crustal thinning event, which 115 culminated in displacement between the Iberian and European plates (Puigdefàbregas & P. 116 Souquet 1986; Vergés & Garcia-Senz 2001). Continental rifting in the Pyrenean domain 117 occurred in response to the counterclockwise rotation of Iberia relative to Europe, coeval with 118 the onset of oceanic spreading in the Bay of Biscay between Chron M0 and A330 119 120 (approximately 125-83 Ma) (Le Pichon et al. 1970; Choukroune & Mattauer 1978; Olivet 1996; Gong et al. 2008; Jammes et al. 2009). About forty metric- to kilometric-sized 121 fragments of subcontinental mantle rocks are found along the northern flank of the Pyrenees, 122 123 in the North Pyrenean Zone (NPZ). They reside within or next to numerous lozenge-shaped basins flanking the North Pyrenean Fault (NPF). These basins are interpreted as the remnants 124 of isolated, pull-apart or transtensive half graben basins formed in response to the eastward 125 drift of Iberia along the NPF and later inverted during the Late Cretaceous-Early Cenozoic 126

Pyrenean orogeny (Le Pichon et al. 1970; Choukroune & Mattauer 1978). A typical flysch
sedimentation started during the mid-Albian within these basins (black flysch), which later
enlarged during the Late Albian and connected into one single, wider basin trough during the
Cenomanian (Debroas 1976; P. Souquet et al. 1985; Debroas 1990).

Various scenarios have been proposed for the emplacement of the ultramafic bodies, ranging 131 from purely tectonic mechanisms, such as solid intrusion of hot or cold mantle rocks into 132 sediments during strike-slip events (Avé-Lallemand 1967; Minnigh et al. 1980; Vielzeuf & 133 Kornprobst 1984), to tectono-sedimentary processes in which mantle rocks were exhumed 134 during Variscan time (Mattauer & Choukroune 1974; Fortane et al. 1986) and reworked in a 135 mid-Cretaceous wild flysch (Fortane et al. 1986). In recent re-examinations, various authors 136 propose that some of these bodies are fragments of sub-continental mantle basement partially 137 exhumed during Albian-Cenomanian times (Lagabrielle & Bodinier, 2008; Jammes et al. 138 139 2009; Lagabrielle et al. 2010; Debroas et al. 2010; Clerc et al. 2012). Within the NPZ, the metasediments are locally strongly deformed and underwent a High Temperature - Low 140 141 Pressure (HT-LP) mid-Cretaceous metamorphic event, which lasted nearly 30 Ma from 110 142 Ma to 80 Ma (Azambre & Rossy 1976; Albarède & Michard-Vitrac 1978b; Montigny et al. 1986; Golberg et al. 1986; Goldberg & Maluski 1988; Thiébaut et al. 1988; Thiébaut et al. 143 1992). This metamorphism is considered as a consequence of crustal thinning (Golberg & 144 Levreloup 1990) and developed in relation with hydrothermal circulations (Dauteuil & Ricou 145 1989). Hydrothermal circulations are also responsible for extensive albitization of some of the 146 North Pyrenean Massifs (Demange et al. 1999; Boulvais et al. 2007; Poujol et al. 2010), and 147 formation of massive talc deposits (Moine et al. 1989; Schärer et al. 1999; Boulvais et al. 148 2006) probably in relation to the activity of major ductile extensive shear-zones (Passchier 149 150 1984; St Blanquat et al. 1986; Costa & Maluski 1988; St Blanquat et al. 1990; St Blanquat 1993). 151

153 III. Geology of the sampling sites

The ophicalcites and related ultramafic breccias selected for the oxygen and carbon isotope study were sampled from peridotite bodies exposed all along the NPZ (fig. 1). We selected nine localities which are representative of the variety of the Pyrenean peridotites, and presumably of the different geological processes involved in their exhumation history. Two sampling sites are located in the western Pyrenees (Urdach and Tos de la Coustette), one in the central Pyrenees (Moncaup) and nine in the Eastern Pyrenees (Ercé-Angladure, Lherz, Fontête Rouge, Freychinède, Berqué, Vicdessos, Urs, Bestiac, Caussou).

161

#### 162 III.1. Western peridotites

163 Several peridotite bodies outcrop in the Chaînons Béarnais, within the fold and thrust belt Mesozoic sequence of the NPZ, at a longitude corresponding to the western termination of the 164 Paleozoic Pyrenean axial zone. The base of the stratigraphic sequence, exposed along the 165 166 Mail Arrouy, Sarrance and Layens post-Cenomanian thrusts (Casteras 1970), is composed of Late Triassic evaporites, breccias and ophites overlain by Mesozoic platform carbonates 167 forming the original cover of the northern Iberian margin (Canérot et al. 1978; Canérot & 168 Delavaux 1986). In contrast to the Eastern NPZ, evidence of HT-LP metamorphism is 169 restricted here to some scarce and narrow regions bordering fault contacts with Triassic and 170 mantle rocks (Fortane et al. 1986; Thiébaut et al. 1992; Lagabrielle et al. 2010) and the 171 temperatures during peak metamorphism barely exceeded 400°C (Clerc 2012). Petrological 172 and geothermobarometric studies of the western ultramafic bodies show that they underwent a 173 two step exhumation with a first rise from 60 km to 25 km depth (1050-950°C), probably 174 during late Hercynian times, followed by a further step from 25 km to a shallower and cooler 175

176 (600°C) level (Fabriès et al., 1998). This second step is marked by the development of a
177 mylonitic fabric, from 117 Ma to 109 Ma (Vissers et al. 1997; Fabriès et al. 1998).

The Urdach body is a 1.5 km wide peridotite slice exposed at the western termination 178 of the Mail Arrouy thrust (fig. 2A). It is overlain by Paleozoic basement slices and surrounded 179 on its western and southern sides by a large volume of unsorted sedimentary breccias and 180 olistoliths composed of peridotite fragments associated with Paleozoic basement clasts from 181 upper, middle and lower crustal levels. These debris are intermingled in the Cenomanian 182 black flysch (Casteras 1970; Vielzeuf 1984; Souquet et al. 1985; Jammes et al. 2009; Debroas 183 et al. 2010). Some authors considered that the Urdach body itself might be an olistolith settled 184 in Cenomanian sediments (Duée et al. 1984; Fortane et al. 1986). Peridotite hydrothermal 185 alteration led to pervasive serpentinization reaching 80%. This is a dominant character of the 186 Urdach body (Fabriès et al. 1998). 187

The 400 m long Tos de la Coustette ultramafic body is located 3 km west of the 188 189 Saraillé summit, at the western termination of the Sarrance anticline (fig 2a). Apart from the peridotites, the faulted heart of the Sarrance anticline includes, Paleozoic basement rocks and 190 ophite lenses embedded within cataclastic Triassic sediments. It is thrusted over the 191 verticalized Urgonian limestones and Albian flysch of the Lourdios Syncline (Casteras 1970; 192 Lagabrielle et al., 2010). The Tos de la Coustette body itself is in tectonic contact with small 193 lenses of Paleozoic crustal rocks and Triassic metaevaporites outcropping both above and 194 beneath the peridotites. Like the Saraillé peridotites, the environment of the Tos de la 195 Coustette body is devoid of sedimentary breccias; instead these bodies are entirely surrounded 196 197 by cataclastic breccias limited by tectonic contacts and are thought never to have been exposed to the seafloor (Canérot & Delavaux 1986; Lagabrielle et al. 2010). 198

#### 200 III.2. Central peridotites

The Moncaup ultramafic body is part of a group of peridotites exposures lying around the 201 Milhas massif, in the central Pyrenees (fig. 1). They are associated with basement rocks, 202 variably brecciated Triassic sediments, ophites and Albian mafic intrusions. They are overlain 203 in tectonic contact by highly metamorphosed Mesozoic marbles (Debeaux & Thiébaut 1958; 204 205 Hervouët et al. 1987; Barrère et al. 1984). Although the peridotites have risen to near surface levels, there is no evidence for sedimentary reworking indicating their exhumation on the 206 basin floor. Indeed, based on their geological setting, it can be deduced that the mantle rocks 207 have remained capped by the Mesozoic marbles together with small slices of continental 208 crust, during their uplift along the detachment fault (Lagabrielle et al. 2010). 209

210

#### 211 III.3. Eastern peridotites:

The eastern Pyrenean peridotites are found within narrow belts of Mesozoic sediments of the 212 NPZ, mainly limestones, pinched between the Axial Zone to the south and blocks of 213 Paleozoic crust to the North representing the continental basement of the NPZ (North 214 Pyrenean massifs) (fig. 1). Although the eastern Pyrenean mantle outcrops are often small and 215 disconnected from an original substratum, one can still observe, on a decametric scale, a 216 progressive transition from carbonate-free massive peridotites to high carbonate content 217 218 breccias with all intermediates. On the rim of the ultramafic bodies, the massive peridotites are often crosscut by millimetric to centimetric calcite veins over the first few meters. In 219 addition, in many localities, the peridotites are reworked within sedimentary polymictic 220 breccias together with highly variable proportions of carbonate clasts. The amount of matrix 221 of these breccias increases toward the carbonated end-member. 222

Most of the ultramafic bodies sampled for this study, from West to East, namely Ercé-223 Angladure, Lherz, Fontête Rouge, Freychinède, Berqué, Vicdessos, Urs, Bestiac and Caussou, 224 display geological settings consistent with an origin as olistoliths surrounded by polymictic 225 226 detritic formation (fig. 2B, 3). They are interpreted as sedimentary records of the exhumation of the peridotites on the floor of the Cretaceous basins (Lagabrielle & Bodinier 2008; Clerc et 227 al. 2012). The ultramafic-bearing breccias show sedimentary features such as grain-sorting 228 and crossbeddings and can be found away from the main bodies, indicating that they have 229 230 been transported by sedimentary processes. Lagabrielle & Bodinier (2008) showed that the polymictic ultramafic-carbonate clastic sediments have been emplaced into fissures opened 231 within the exhumed massive peridotites, in a way similar to OC2 sedimentary ophicalcites of 232 Lemoine et al. (1987). Similar features are reported in more detail, together with the presence 233 of ultramafic-rich debris flows and evidence of ultramafic rock-fall in the vicinity of the 234 235 Lherz body by Clerc et al. (2012). The peridotites show little serpentinization, developed mainly along discrete, localized joints and fissures. The carbonates reworked in the detritic 236 237 formations surrounding the peridotites are strongly deformed and underwent HT-LP 238 metamorphism with peak temperatures commonly as high as 600°C (Golberg & Leyreloup, 1990; Clerc 2012). By contrast to the western peridotites, the eastern ones underwent a single 239 and rapid uplift event, which probably limited hydrothermal alteration and serpentinization 240 (Albarède & Michard-Vitrac 1978a; Fabriès et al. 1991; Henry et al. 1998). 241

242

# 243 IV. Description of the analyzed samples

## 244 IV.1. Sampling strategy and collected samples

The sampling strategy was to collect samples from the four main geological environments identified and distinguished as follows: (1) poorly serpentinized peridotites surrounded by hot

metasediments (Eastern and central peridotites) either exhumed to the basin floor (Lherz, 247 Bestiac, Caussou, Vicdessos, Urs, Ercé-Angladure) or only unroofed but never exhumed 248 (Moncaup), and (2) highly serpentinized peridotites surrounded by cooler sediments (Western 249 250 peridotites) either exhumed to the basin floor (Urdach) or only unroofed but never exhumed (Tos de la Coustette). The list of the 48 studied samples is given in Table 1. We focused this 251 study on the Lherz and Urdach bodies since they are among the largest mantle outcrops in the 252 Pyrenees and because they represent two well-studied end-members in terms of their 253 geological environment. Furthermore, these two localities offer better outcrop conditions 254 compared with the smaller bodies poorly exposed in areas presenting important vegetal 255 256 covering and rock alteration.

#### 257 IV.2. Field and macroscopic aspects:

#### 258 IV.2.a. Western Pyrenean Ophicalcites:

259 The western ophicalcites appear essentially as veins of calcite infilling fissures and fractures opened within the ultramafic rocks. The fractures present relatively constant and repeated 260 orientations (fig. 4A). Particularly well observable in a quarry opened on the western side of 261 262 the Urdach lherzolite body, they were first described by Monchoux (1970) and later interpreted as typical ophicalcite textures by Jammes et al. (2009). These authors highlighted 263 their similarities with structures observed within exhumed mantle in the Alps and drilled off 264 Iberia (Manatschal 2004). They consist mainly in millimetric to decimetric veins of clear 265 white calcite (fig. 4B). The thickest veins are actually constituted of an accumulation of 266 numerous veins and veinlets separated by thin fragments of peridotite strapped from the rims. 267

At Tos de la Coustette, the ophicalcites also appear as a dense mesh of very fine veinlets and as a pervasive substitution of serpentine minerals by patches of carbonate, barely visible on a macroscopic scale, invading highly serpentinized peridotites (fig. 4C and D). Similar textures
have also been described further east in the Avezac-Moncaut peridotites (Fabriès et al. 1998).

#### 272 <u>IV.2.b. Central Pyrenean Ophicalcites:</u>

273 At least two types of ophicalcites were identified in the Moncaup peridotites. The first one, observed close to the damage zone of the tectonic contact between the peridotites and the 274 overlying marbles, is represented by millimetric veins of coarse translucent sparite (fig. 4E). 275 The veins crosscut and hence post-date a mylonitic fabric affecting the peridotites. The 276 second one, observed in the damage zone of the detachment fault, consists of light brown 277 micro-conglomerates and micrite infilling veins and cavities opened in the altered and 278 dislocated peridotites (fig. 4F). The cavities present contorted and rounded rims. The micro-279 sediments show complex multi-generation evolutions with successive stages of deposition 280 281 indicated by several color shades and crosscutting sparitic veins. The micro-conglomerates are laminated and present clear grain-sorting. 282

#### 283 IV.2.c. Eastern Pyrenean Ophicalcites:

In the Eastern Pyrenees, ophicalcites and polymictic ultramafic-marble bearing breccias are observed within, close to, and even far away from the main peridotite bodies. Most of the clasts are composed either of ultra-fresh subcontinental peridotites or of marbles bearing mineral assemblages typical of the HT-LP mid-Cretaceous metamorphism. They are associated with a minor proportion of fragments deriving from gabbros, Triassic ophites Mesozoic meta-pelites and meta-evaporites and Paleozoic basement rocks (Lagabrielle & Bodinier 2008; Clerc et al. 2012).

In the Etang de Lherz area, Lagabrielle and Bodinier (1998) identified four main types of breccias and ophicalcites that can be extended to the other peridotite outcrops of the Eastern Pyrenees. (i) Type 1 is found in direct contact with or within the ultramafic body, it consists

of a carapace of monomictic breccias resulting from the cataclastic deformation of the 294 peridotites during exhumation. These breccias typically lack carbonate clasts and contain little 295 to no carbonate veins and cement. Therefore, they will not be considered further in this study. 296 (ii) Type 2 breccias, generally found in close contact with type 1 breccias, are ultramafic-297 dominated polymictic breccias resulting from the sedimentary reworking of type 1. (iii) Type 298 3 breccias consist of thin layers of graded ultramafic litharenites bearing isolated cm-sized 299 clasts of peridotites and marbles and presenting slumps and syn-sedimentary normal faults 300 (fig. 5A and B). Within the type 3 breccias, the peridotite clasts display many different 301 lithologies (lherzolite, harzburgite, websterite, pyroxenite etc.), variable mantle textures 302 303 (equant coarse-granular to mylonitic) and variable degrees of serpentinization (totally fresh to fully serpentinized, fig. 5C and D). These observations point to mixing and transport from a 304 relatively distant source by sedimentary processes. Furthermore, clasts of former monomictic 305 carbonate breccias and polymictic UM-marble breccia are also reworked in these formations, 306 pointing to their late deposition with regard to the exhumation history (Clerc et al., 2012). (iv) 307 308 Type 4 breccias correspond to clastic rocks closely resembling the OC2 sedimentary ophicalcites of Lemoine et al. (1987). Clear white calcite veins penetrate fractured ultramafic 309 blocks in which they separate angular fragments. There is a striking association of these veins 310 with matrix-supported microbreccias similar to those forming the matrix of the type 2 breccias 311 (fig. 5E). The veins are smoothly rooted in the matrix and seem to be its extension in narrow 312 domains where the clasts were too big to fit. However, some veins crosscut pre-existing 313 matrices, pointing to a contemporaneous formation of matrices and veins during 314 315 sedimentation accompanied by multi-stage circulations of cementing fluids. In some outcrops, the ultramafic clasts exhibit a centimeter thick orange-brown oxidation ring on their contact 316 317 with carbonate matrices and veins (fig. 5 E and F). This feature is also commonly observed in oceanic ophicalcites (Boschi et al. 2006; Dick et al. 2008). This oxidation pattern does not 318

319 appear on the rims of the thinnest veins.

Ophicalcites at the Bestiac locality show similar features and offer exceptional 320 conditions to investigate the successive generations of serpentinization and carbonation. The 321 peridotite consists of tens of lens-shaped bodies less than a few hundred meters in size and 322 embedded in a metamorphic bimodal ultramafic-marble breccia. Angular to slightly rounded 323 centimeter-sized clasts of lherzolite are found more than 500 m away from the main blocks, a 324 pattern clearly not consistent with any fault-assisted mode of emplacement. A few outstanding 325 outcrops are visible in several abandoned caves and galleries dug for prospection of asbestos. 326 Fresh to dark green serpentinites are crosscut by networks of cm-thick light green fibrous 327 328 serpentine (likely chrysotile) delimitating metric lumps which mimict at a meter-scale the classical microscopic mesh-texture of serpentinized peridotites (Wicks & Whittaker 1977) 329 (fig. 5G). The serpentine veins commonly show oblique sigmoidal fibers indicating shearing 330 331 contemporaneous to brittle deformation responsible for vein development. Pluri-millimetric veins of calcite crosscut through this latest generation of serpentine veins that acted as a weak 332 333 gateway for sediments and fluids during the ultimate stage of deformation and sedimentary 334 reworking (fig. 5H). Some of the calcitic veins have a reddish coloration and increased concentration of oxides, suggesting possible syn- or post-diagenetic hydrothermal circulation. 335 As in the Lherz area, these remarkable ultramafic-bearing formations have a relatively 336 restricted extension and appear within large volumes of clastic formations devoid of any 337 ultramafic component. 338

339

#### 340 IV.3. Microscopic description:

Ophicalcite from the Urdach ultramafic body have millimetric veins of sparite. Several veingenerations crosscut each other with varying angles. The calcite veins commonly show crack-

seal aspects. Symmetric layers of calcite with varying intensity in transmitted light and
cathodoluminescence (CL), induced by minor variations of composition or inclusion
concentration, are separated by a central suture (fig. 6A). Some of the largest veins actually
consist of an accumulation of numerous sub-parallel veinlets, less than a micrometer wide,
invading the serpentinite (fig. 6B). Finally, some other veins show zonated botryoids of
fibrous radiating calcite (fig. 6C)

In the Tos de la Coustette ophicalcites, the carbonates mainly appear as micrometric to millimetric patches of calcite extensively dispersed within the serpentinite (fig. 6D). Intimate repartition of calcite and serpentine indicate a pervasive calcification by replacement of some serpentinous phases. The poorly elongated calcite aggregates develop following a general foliation marked by magnetite alignments and thin yellow serpentine veinlets. Surface estimate by digital image treatment indicates that the rock includes up to 55 % calcite, 40 % serpentine and 5 % magnetite with minor phases.

The matrix of the eastern Pyrenean ophicalcites and associated polymictic breccias consists of 356 a pale-orange litharenite composed of infra-millimeter-sized angular clasts of marbles mixed 357 with varyingly serpentinized ultramafic clasts and isolated minerals (pyroxenes, olivine, green 358 and brown spinels). This litharenite sometimes appears laminated and shows graded-bedding 359 due to sedimentary transport (Lagabrielle & Bodinier 2008; Clerc et al. 2012) (fig. 6E). In 360 contrast to the veins, the matrices of the breccias, show much less evidence for 361 recrystallization: there are, for example, a few newly formed metamorphic phyllosilicates and 362 amphiboles. 363

Most of the veins observed in the Eastern Pyrenean ophicalcites consist of clear and equant sparry calcites (fig. 6F). The veins cross cut alternatively the ultramafic clasts and the matrix of the breccias in which they often seem to be rooted. In the simplest cases, a single

generation of calcite crystal nucleates from the rims of the veins and grows toward the center 367 where it joins in a central suture. In some cases, the growth resumed or the fracture was 368 reopened, leading to the formation of vugs. Most of the veins show multistep histories with 369 370 successive infillings of sparite particularly well highlighted by varying luminescence in CL (fig. 6G). When pure enough, the veins are clearly recrystallized as evidenced by the 371 conservation of former zoned calcite dogteeth ghosts within bigger equant neoformed 372 crystals. The borders of the neoformed crystals are independent from those of the ghosts that 373 374 they overprint (fig. 6H). When thick enough, the veins are generally filled with detrital material including micro-fragments of serpentine, oxides and calcite clasts mixed within a 375 micrite. Although they lack microfossils, such veins resemble the neptunian dykes and veins 376 formed on the subaquatic floor and consequently opened to sedimentary influx (Smart et al. 377 1987; Laznicka 1988; Winterer et al. 1991). 378

#### 379 V. Methods for determination of O and C isotope compositions

Rock samples were sawed to select well-oriented and relevant planes. The sawed faces were
cleaned using water and pulsed with dry air before micro-drilling. A minimum of about 20 mg
of powder was collected for each sampling site.

The O and C isotope compositions were measured using a VG SIRA 10 triple collector mass 383 spectrometer at the University of Rennes 1, on the CO<sub>2</sub> released during reaction of calcite 384 with anhydrous H<sub>3</sub>PO<sub>4</sub> in sealed vessels at 50°C (McCrea 1950). NBS 19 and internal-lab 385 standard references materials (Prolabo Rennes) were continuously measured during the course 386 of this work. NBS 19 measured values were  $\delta^{18}O = 28.26 \pm 0.09$  (1 $\sigma$ , n=12) ‰ and  $\delta^{13}C =$ 387  $1.86 \pm 0.02$  (1 $\sigma$ , n=12) ‰. Results were corrected in accordance with the NBS 19 388 recommended values of 28.65‰ and 1.95‰, for O and C respectively. The analytical 389 390 uncertainty is estimated at 0.15‰ and 0.1‰ for O and C.

## 391 VI. Results

The isotope compositions for the 48 analyzed samples are presented in table 1 and figure 7. 392 The calcite phase found in clasts, veins and matrices from the Pyrenean ophicalcites and 393 ultramafic-bearing breccias displays a wide range of oxygen isotope compositions with 394 minimum values of 12.6 and 13.8‰ (vs. SMOW) measured in Moncaup and Tos de la 395 Coustette veins (Western ophicalcites), and maximum values of 25.1‰ in the matrices of 396 samples from Etang de Lherz area (fig. 4 & 6; Eastern ophicalcites). The carbon isotope 397 398 compositions range from -5.8‰ (vs. PDB) in Moncaup samples to 1.5‰ in Lherz samples (matrices). As a whole, the field of isotopic compositions of Pyrenean ophicalcites is 399 displaced from the one of the Iberian margin ophicalcites by lower  $\delta^{18}$ O values and slightly 400 lower  $\delta^{13}$ C values (arrow in figure 7). Whereas no clear distinction can be made when 401 comparing Pyrenean ophicalcites with Alpine and Apenninic ones, it seems that hydrothermal 402 ophicalcite worldwide compare well with ophicalcites from the Western Pyrenees. First order 403 analysis of the distribution of the oxygen and carbon isotope compositions implies to 404 distinguish two separate domains: i) Ophicalcites from the Urdach and Tos de la Coustette 405 ultramafic bodies have rather low and variable values of  $\delta^{18}$ O and  $\delta^{13}$ C, ranging from  $\delta^{18}$ O = 406 13.8 to 22.1‰ and  $\delta^{13}$ C = -5.22 to 1.12‰ and scattered around a mean value of  $\delta^{18}$ O = 19.1‰ 407 and  $\delta^{13}C = -1,0\%$ . Ophicalcites from Tos de la Coustette body plot into a distinct field having 408 an extremely low value of  $\delta^{18}$ O. ii) Ophicalcites from the Eastern Pyrenean bodies display 409 low dispersion (21.3 to 25.1‰) in  $\delta^{18}$ O but variable  $\delta^{13}$ C values (1.53 to -2.47‰). Among the 410 Eastern Pyrenean ophicalcites, very poor discrimination can be made based on the 411 composition of veins and matrices since both display almost similar values with mean  $\delta^{18}$ O of 412 23.4‰ in the veins and 24.1‰ in the matrices. The O and C isotope compositions of the nine 413 samples containing both veins and matrices are reported in figure 8. One can observe good 414 correlations between the compositions of matrices and veins with the exception of samples 415

LHZ8 and LHZ64 whose veins are significantly depleted in <sup>18</sup>O and slightly enriched in <sup>13</sup>C. 416 We note that the pluri-millimetric size of our sampling drilling spots provide bulk estimates of 417 the isotopic compositions of the veins and matrix but do not allow the complex multistage 418 history recorded in some of the veins to be deciphered (i.e. fig. 6G). The isotope composition 419 of the matrices does not correlate with the variable lithology of the clasts (either ultramafic 420 and/or carbonate), nor with the relative amount of clasts. In contrast the isotopic compositions 421 of the marble clasts are highly variable and plot within a larger field than the matrices and 422 veins (Fig. 7). Also, there is no correlation between the isotopic compositions of clasts and the 423 veins or matrices that host them. Actually, these clasts underwent a strong HT/LP 424 metamorphism and may contain abundant silicates (phyllosilicates, amphiboles, scapolite). 425 Closed-system isotopic equilibration between the carbonate and the silicate phases likely 426 introduced variable isotopic alteration of the carbonate phase, depending on the initial amount 427 428 of detrital silicates in the sedimentary precursor (see for example Valley, 1986; Boulvais et al., 2000). Also, open-system alteration during syn-metamorphic infiltration possibly caused 429 430 isotopic shifts, which remain difficult to estimate here because we have no more information 431 on the initial geometry of the clast (for example the distance to a lithological discontinuity). The ophicalcites from the Moncaup body display two distinct generations of carbonates with 432 distinct isotopic compositions (fig. 4C and D). Such differences in isotopic compositions are 433 consistent with the occurrence of two types of textures as described in section IV. 434

435

# 436 VII. Discussion

437 VII.1. Origin of the various types of ophicalcites

Based on the petrographic descriptions on the one hand and on the stable isotope
compositions on the other, we are able to distinguish three main categories of ophicalcites
associated with the subcontinental mantle bodies of the northern Pyrenees (table 2).

The first type of ophicalcites or hydrothermal type, as defined in the Tos de la Coustette body 441 results from peridotite carbonation by veins and pervasive substitution of the serpentinite 442 minerals by low  $\delta^{18}$ O calcite. The low  $\delta^{18}$ O values of calcite indicate that carbonation 443 occurred from rather hot fluids. Comparable  $\delta^{18}$ O values have been measured in ophicalcites 444 formed in oceanic and ophiolitic hydrothermal systems (Lavoie & Cousineau 1995; Artemyev 445 & Zaykov 2010). Due to its low  $\delta^{18}$ O, the first generation of coarse crystalline calcite veins 446 described in the Moncaup peridotite likely corresponds to this type of hydrothermal 447 448 ophicalcite. The difference in texture types between the Moncaup and the Tos de la Coustette ophicalcites may be explained by the very different rheology and chemical response to fluid 449 circulation of the unserpentinized peridotite at Moncaup compared with the totally 450 451 serpentinized peridotite of Tos de la Coustette.

The second type of ophicalcites or *tectonically-controlled* type is well characterized in the 452 Urdach body. It consists of massive serpentinized peridotites, indifferently lherzolite or 453 harzburgite, crosscut by successive generations of millimetric to centimetric calcite veins with 454 intermediate isotopic compositions. The tectonic control of calcite crystallization is 455 documented by the distribution of veins along preferential planes and their crack-seal 456 geometry. Such calcite crystallizations likely record the arrival of the peridotite close to 457 seafloor environments, directly under the influence of waters with intermediate temperature. 458 Different generations of veins cross-cutting each other with slight variations in isotopic 459 460 composition may reflect some temperature variations during the successive steps of fracturing / precipitation. In sample URD 1, a first generation of vein with a lower  $\delta^{18}$ O values 461  $(\delta^{18}O=18.6\%)$  is cut by a later generation with a higher  $\delta^{18}O$  value ( $\delta^{18}O=21.1\%$ ). This is 462

463 consistent with cooling during vein formations, in consequence of progressive exhumation,
464 provided that the isotopic composition of the invading fluid, and then its source, remained
465 constant throughout the history of this sample.

The third type of ophicalcites, dominant in the eastern Pyrenees, is sedimentary ophicalcite. It 466 consists of a cogenetic association of calcite vein and polymictic breccias. The matrix-467 supported to clast-supported polymictic breccias are composed of variable proportions of 468 marbles and UM clastic material. Polymictic compositions and typical sedimentary features 469 such as grain-sorting and cross bedding indicate that these ophicalcites have a sedimentary 470 origin (Clerc et al., 2012). Their wide lithological variety, both in UM and metasedimentary 471 material, likely results from sedimentary transport and mixing. By analogy with neptunian 472 473 veins observed in other extensional settings (Winterer et al. 1991), the micrite-filled brittle fractures have been interpreted as very late, near surface fracturing of the exposed ultramafic 474 basement (Lagabrielle & Auzende 1982; Morgan & Milliken 1996), possibly leading to 475 476 gravitational instabilities: slumping, slope failure, and landslides as described at ODP site 899 by Gibson et al. (1996). The sparite-filled veins and veinlets, either reworked in the breccias, 477 smoothly rooted in the matrix or crosscutting clasts and matrix reveal a multistage deposition 478 history, already implied by the presence of breccias clasts reworked in the breccias (Clerc et 479 al. 2012). Bernoulli & Weissert (1985) describe similar cogenetic and simultaneous sediment 480 infillings and calcitic cement precipitation in Alpine ophicalcites. Such fractures must have 481 allowed the circulation of sedimentary fluids or early diagenetic fluids in domains where 482 restricted dimension hindered the penetration of sedimentary material. The isotopic 483 compositions of matrices and veins (Fig. 8) show a good correlation in both the oxygen and 484 carbon systems, which confirm the idea that both features developed from the same reservoir. 485 Since the relationship is valuable on a rather large range of  $\delta^{18}$ O and  $\delta^{13}$ C, one can infer that 486

the system of vein + matrix development was not connected to an external reservoir which
would have produced veins with distinct compositions from the ones of the matrices.

Precipitation of acicular aragonite has commonly been correlated with warm water 489 temperatures, high Mg/Ca ratios, high salinity, and high carbonate concentrations, conditions 490 reached in the uppermost levels of serpentine seamounts (Haggerty 1987; Lagabrielle et al. 491 1992). Similar thermal and chemical conditions are associated with fibrous, botryoidal calcite 492 occurrences (Folk 1974; Surour & Arafa 1997), and botryoidal calcite could also represent a 493 replacement texture of acicular radiating aragonite (Ross 1991). More equant and bladed 494 sparry calcite has been correlated with cooler, deeper marine or meteoric settings, typically 495 with low Mg, and carbonate concentrations (Folk 1974; Burton & Walter 1987). Instead, 496 497 geochemical data (trace element and isotopic signatures) from Iberian margin ophicalcites indicate a seawater imprint at temperatures of 10-20°C, consistent with an early Cretaceous 498 seawater only slightly modified by interaction with serpentinized peridotite basement 499 500 (Milliken & Morgan 1996). For that reason, Morgan & Milliken (1996) suggested that the 501 temporal evolution in the carbonate phase and morphology, from precipitation of aragonite, followed by fibrous, botryoidal calcite and finally to coarse, bladed sparry calcite may be 502 controlled primarily by fluid flow rates through the vein rather than by variations of the 503 chemical and thermal parameters (fig. 9). 504

The low temperature ophicalcites from the Moncaup body (MP84a, b, c) are peculiar in that they have extremely low  $\delta^{13}$ C (< -5.00 ‰), indicative of interaction with organic material. Such carbon isotope compositions are commonly observed in karstic or calcrete precipitations from continental/meteoric waters transiting through soils and vegetation. These peculiar ophicalcites are located immediately below the cataclastic formations staking out the detachment fault between the peridotites and the overlying marbles. Due to the solubility and permeability contrast between these two formations, this interface is prone to concentrating groundwater. However, we cannot specify if the formations observed are contemporaneous of any very early exhumation of the mantle rocks to subaerial (onland) environments in the Cretaceous or if they result from a later karstification and/or replacement of pre-existing ophicarbonates. Regardless the exact explanation, these values strongly differ from the rest of our dataset by a clear shift toward lower  $\delta^{13}$ C values, allowing the distinction to be made between a surface-derived cement precipitated in karstic environments and sedimentary ophicalcites deposited in subaqueous conditions.

# 519 <u>VII.2. Environmental conditions for the formation of Central and Eastern Pyrenean</u> 520 <u>ophicalcites</u>

The isotopic compositions of the Pyrenean ophicalcites fall into the same field as other 521 ophicalcites from the literature (fig. 7). Only the three samples from Moncaup MP84a, b, and 522 c are out of this range because of their low carbon composition indicative of interactions with 523 carbon from soils, as discussed above. Ophicalcites from the Alps and Apennine were 524 interpreted as having been formed by interaction with seawater moderately heated to 80 to 525 less than 200°C (Barbieri et al. 1979; Barrett & Friedrichsen 1989; Früh-Green et al. 1990; 526 Schwarzenbach 2011) or by sedimentary fluids later re-equilibrated during Alpine 527 metamorphism (Weissert & Bernoulli 1984; Barbieri et al. 1979). 528

Samples from the Eastern Pyrenees are clearly recognized as sedimentary ophicalcites by their textures. Consistently, the Eastern Pyrenean ophicalcites have the highest  $\delta^{18}$ O values measured in our sample set, a feature which is indicative of low temperatures of precipitation at near surface conditions. However, we notice a major difference in the oxygen isotope composition with ophicalcites from the Iberian margin (Agrinier et al. 1988; Evans & Baltuck 1988; Agrinier et al. 1996; Milliken & Morgan 1996; Plas 1997; Skelton & Valley 2000). Indeed, in the Iberian ophicalcites, which precipitated from low temperature seawater, the 536  $\delta^{18}$ O values of calcite are around 31‰ with  $\delta^{13}$ C values varying between -1.7 and 2.2‰. 537 Instead, the Eastern Pyrenean sedimentary ophicalcites analyzed in our study have 538 significantly lower  $\delta^{18}$ O values (around 24‰) with carbon isotope compositions ranging from 539 -2.5 to 1.4‰, so that even if the envelope of Pyrenean sedimentary ophicalcites mimic the 540 Iberian margin ones, it is displaced in the  $\delta^{13}$ C vs.  $\delta^{18}$ O space (grey arrow, fig. 7). At least, 541 three hypotheses can be proposed in order to explain these differences (fig. 10).

542 1. Lowering of the O and C isotope compositions could result from a metamorphic imprint with introduction of externally-derived fluids. Isotopic exchanges between neoformed calcites 543 and the mineral silicates, mainly serpentinite, which form a significant portion of the detrital 544 545 material associated with the sedimentary ophicalcites, may lower the O isotope composition 546 of the calcite. The breccias and ophicalcites rework clasts of pre-rift material that already bear signs of high-grade recrystallization during the regional HT/LP metamorphism, with the 547 548 development of scapolite and amphibole. The deposition of the breccias and ophicalcites hence occurs after the peak of metamorphism. But the long-lasting mid-cretaceous thermal 549 anomaly is followed by a lower grade metamorphism that affects the Turonian-Senonian post-550 rift sediments, with a maximum temperature near 350°C (Ternet et al., 1997; Clerc 2012). 551 This later and lower grade metamorphism may hence have affected the ophicalcites and 552 553 breccias presented in this study. However, the petrographical effect of metamorphism on these rocks seems rather limited since the matrices show only little recrystallization. 554 Furthermore, we would expect that the oxygen isotope composition would be much more 555 556 variable depending on the fluid/rock ratio. This is the case for a metamorphic-driven alteration of the isotopic signal as shown from the study of the Alpine ophicalcites (Fig. 7; 557 558 Weissert & Bernoulli 1984; Früh-Green et al. 1990). Also, one would have expected that the veins show more constant composition instead of displaying delta values that correlate with 559 the values of matrices (Fig. 8). 560

2. The low O and C compositions may be the result of a hot diagenesis from marine porewater 561 during carbonation. This hypothesis, which implies active circulation of relatively hot fluids 562 in the boundary layer between the ultramafic basement and seawater, is consistent with the 563 high geothermal gradients known to characterize the basins of the North Pyrenean Zone 564 during the Albian-Cenomanian period (Dauteuil & Ricou 1989; Golberg & Leyreloup 1990). 565 The thermal gradients for the Albo-Cenomanian metamorphism can be higher than 100°C/km. 566 In such conditions, we may also consider that unconsolidated sediments still soaked with 567 568 seawater can be rapidly buried and heated to temperatures as high as 50-80°C. At such temperatures, the calcite precipitated from seawater ( $\delta^{18}O = 0\%$ ) would have a  $\delta^{18}O$  value of 569 around 23% (considering the isotopic fractionation coefficient of Zheng, 2011), a value that 570 compares well with the data of the Eastern ophicalcites. Thermal gradients as high as 160-571 180°C/km are known in present days, for instance in the Salton Sea geothermal field (Elders 572 573 et al., 1972; Muffler & White, 1969). Comparable environments can also be found on the top of mantle exhumed in oceanic domains, where hydrothermal fields develop over areas several 574 square kilometerswide (around 2.5km<sup>2</sup> at the Rainbow hydrothermal site, German et al., 1996; 575 around 2km<sup>2</sup> at the Lost City hydrothermal site, Kelley et al., 2001, along the Mid-Atlantic 576 Ridge). In similar settings, in the ophiolites of East Liguria, Spooner and Fyfe (1973) describe 577 temperatures as high as 400°C for shallow depth of circa 300 m below the water/rock 578 579 interface.

3. As a last hypothesis, it may be that the Eastern Pyrenean sedimentary ophicalcites formed in a low-temperature but endorheic environment, dominated by continental waters and possibly disconnected from the ocean. Indeed, the oxygen composition measured here is about 7‰ lower than the present-day marine Iberian ophicalcites, a difference consistent with the difference between marine and unspecific waters with a continental affinity. Note first that a continental environment is not precluded by the existence of marine fauna, which would

have been observed in sediments associated with ophicalcites. The hypothesis of an endorheic 586 environment dominated by continental waters has to be questioned with respect to the 587 paleogeographic reconstructions of the Pyrenean realm during mid-Cretaceous times. These 588 589 reconstructions point to the existence of a V-shape opening oceanic domain, narrowing from the Bay of Biscay toward the East where it propagates into the continental crust (Jammes et 590 al. 2009 and references therein). The opening of numerous transtensive basins of limited 591 extension in the central and eastern part of the pre-Pyrenean domain may have been such that 592 593 these basins were endorheic (Le Pichon et al. 1970; Choukroune & Mattauer 1978), partially disconnected from a marine influence at the time of ophicalcite development. This hypothesis 594 is consistent with the stratigraphy of the Albian sediments deposited in disconnected basins 595 separated by positive reliefs (Debroas, 1976, 1990; Souquet et al., 1985). Some of these 596 reliefs such as the future North Pyrenean massifs and the future Axial Zone were emerged, as 597 598 shown by the outline of the Cenomanian transgression and by evidence of cooling and sedimentary reworking of crustal material (Filleaudeau et al., 2011). Such short wave-length 599 600 and high amplitude morphology likely resulted from the flexural response of the lithosphere 601 to the extreme crustal stretching due to the extensional Albian-Cenomanian tectonics along the Pyrenean realm. In such conditions, we may envision that the area where mantle has been 602 exhumed was surrounded by subaerial catchments and, at that time possibly disconnected 603 from the sea. A possible present-day analog is represented by the Salton Sea basin, which is 604 an endorheic continental basin located ahead of the propagating oceanic spreading axis of the 605 Gulf of California. Circulations of continental waters within sediments are also described in 606 607 more opened environments, for example at the foot of the Aden Gulf margins (Lucazeau et al. 2010). 608

At this time, it is difficult to select between the three hypotheses even if the last one is the simplest in term of the isotopic composition record. Additional informations like fluid 611 inclusion data is needed to strengthen this hypothesis. It remains clear that, regardless of the
612 exact explanation, sedimentary ophicalcites in the Eastern Pyrenees are distinguishable from
613 those in the Central and in the Western Pyrenees.

#### 614 VII.3. Western and Eastern Pyrenean ophicalcites: why are they so different?

615 The three types of ophicalcites identified in this study have to be considered within the frame 616 of the exhumation history of the Pyrenean peridotites presented in section III a and c and as summarized in figure 11. We highlight a clear distinction between the Eastern and Western 617 Pyrenean isotope composition of ophicalcites also evidenced by the different degrees of 618 619 serpentinization of the mantle that host them, by the temperatures of the metamorphic peak in the surrounding metasediments (Choukroune & Seguret, 1973; Golberg & Leyreloup, 1990; 620 Ravier, 1959; Clerc 2012) and by the typologies of ophicalcites (fig. 11). Following our 621 622 observations, and in accordance with phase stability of serpentine mineral (Andreani et al. 2007), it appears that the variable serpentinization degree of the Pyrenean peridotites can be 623 linked, primarily, to the thermal anomaly accompanying their exhumation. Since carbonation 624 postdated serpentinization, the degree of serpentinization appears as a key factor influencing 625 the development of ophicalcites. Volume increase and rheological softening induced by 626 627 serpentinization tend to favor the development of numerous fractures, allowing an endogenic precipitation of carbonates as observed in the Western ophicalcites. In contrast, the less 628 serpentinized peridotites exposed in Moncaup and in the Eastern Pyrenees must have had a 629 different behavior during uprising to crustal levels. Their contrasting rheology with the 630 surrounding rocks implies that they were probably still massive and competent until 631 exhumation. This could explain the predominance of superficial ophicalcites found in these 632 633 localities. The fact that the Eastern Pyrenean peridotites remained preserved from hydrothermal circulation may explain their scarce serpentinization. In addition, such a lack of 634 fluid activity may also be responsible for the preservation of high temperature mineral 635

assemblage since heat was evacuated by convection. The reason of the limited access of fluids
to the exhuming peridotites is not yet understood. We could suggest either i) a blanketing
effect of the Mesozoic sedimentary cover that would inhibit water infiltration, or ii) fast
exhumation in a continental environment with limited amounts of water available for
hydrothermal circulations.

641

#### 642 <u>Conclusion</u>

643 On the basis of close fieldwork, petrographic and geochemical considerations, we present the first comprehensive review of the Pyrenean ophicalcites. Our results, in accordance with 644 published studies on worldwide occurrences of ophicalcites allowed us to distinguish and 645 characterize three main types of ophicalcite (table 2): (i) hydrothermal ophicalcites resulting 646 in low  $\delta^{18}$ O calcite (13.8‰) pervasively replacing serpentinite; (ii) intermediate or syn-647 648 tectonic ophicalcites developed along with brittle discontinuities in the serpentinized mantle rocks, with intermediate calcite isotope compositions ( $\delta^{18}$ O around 20.0%;  $\delta^{13}$ C around -649 1.06‰); (iii) sedimentary ophicalcites occurring as breccias and neptunian dykes, associated 650 651 with the circulation of syn-sedimentary fluids. The isotopic compositions for this sedimentary type show the highest  $\delta^{18}$ O and  $\delta^{13}$ C values of the set, consistent with the cold temperatures of 652 precipitation expected in a sedimentary environment. We note a non-linear distribution of the 653 different ophicalcite type along the Pyrenean range, with dominant endogenic ones in the 654 West and dominant exogenic ones in the East. Such a distribution is clearly linked to a 655 656 difference in serpentinization degrees likely related to the different exhumation histories and subsequent variable thermal anomalies. 657

We further investigated the possible origins of the fluid and temperatures at which the calcite may have precipitated in both hydrothermal and sedimentary domains. We present three

possible explanations for the relatively low values of the sedimentary ophicalcites: i) a post-660 sedimentary metamorphic imprint; ii) a hot diagenesis in relation to the high regional thermal 661 gradient; iii) sedimentation in an endorheic basin. This last hypothesis is consistent with the 662 paleogeographic reconstructions of isolated Albo-Cenomanian basins at the tip of a 663 propagating rift. Finally, we highlight a major difference between Eastern and Western 664 ophicalcites, linked primarily to the variable degree of serpentinization. Considering the 665 strong control of serpentinization on the rheology of mantle rocks we propose that the 666 667 formation of different ophicalcites types is controled by the degree of serpentinization, depending itself on the rate and modalities of exhumation of the subcontinental mantle during 668 669 extreme crustal stretching.

# 671 Acknowledgments:

673	This work was made possible thanks to CNRS, Total, and the Action Marges research group	
674	(INSU, Total, IFP, BRGM, IFREMER) through a Ph.D. grant to C. Clerc. We thank G. Früh-	
675	green and G. Manatschal for their valuable comments that helped improve the quality of the	
676	manuscript. We are grateful to B. Smith for improving the English, to JC. Ringenbach and	
677	Benoit Ildefonse for fruitful discussions and improvement on the quality of the figures, and to	
678	C. Nevado for the high quality thin-sections realized at the Géosciences Montpellier	
679	laboratory.	
680		
681		

- Abbate, E., Bortolotti, V., & Passerini, P. (1970). Olistostromes and olistoliths. *Sedimentary Geology*, 4(3-4), 521-557. doi:10.1016/0037-0738(70)90022-9
- Agrinier, P., Cornen, G., & Beslier, M. O. (1996). Mineralogical and oxygen isotopic features
  of serpentinites recovered from the ocean/continent transition in the Iberia abyssal
  plain. In R. B. Whitmarsh, D. S. Sawyer, A. Klaus, & D. G. Masson (Éd.), *Proceedings of the Ocean Drilling Program, 149 Scientific Results* (Vol. 149, p. 541-
- 691 552). Ocean Drilling Program.
- Agrinier, P., Mével, C., & Girardeau, J. (1988). Hydrothermal Alteration of the Peridotites
  Cored at the Ocean/Continent Boundary of the Iberian Margin: Petrologic and Stable
  Isotope Evidence. In G. Boillot, E. L. Winterer, & et al. (Éd.), *Proceedings of the*
- 695 *Ocean Drilling Program, 103 Scientific Results* (Vol. 103, p. 225-234). Ocean Drilling
- 696 Program. Consulté de http://www-odp.tamu.edu/publications/103\_SR/103TOC.HTM
- Albarède, F., & Michard-Vitrac, A. (1978a). Datation du métamorphisme des terrains
  secondaires des Pyrénées par des méthodes Ar-Ar et Rb-Sr. Ses relations avec les
  péridotites associées. *Bulletin de la société géologique de France, XX*(7), 681-688.
- 700 doi:10.1016/ 0012-821X(78)90157-7
- Albarède, F., & Michard-Vitrac, A. (1978b). Age and significance of the North Pyrenean
  metamorphism. *Earth and Planetary Science Letters*, 40(3), 327-332.
  doi:10.1016/0012-821X(78)90157-7
- Andreani, M., Mével, C., Boullier, A.-M., & Escartín, J. (2007). Dynamic control on
   serpentine crystallization in veins: Constraints on hydration processes in oceanic
   peridotites. *Geochemistry Geophysics Geosystems*, 8(2). doi:10.1029/2006GC001373

- Artemyev, D. A., & Zaykov, V. V. (2010). The types and genesis of ophicalcites in Lower
   Devonian olistostromes at cobalt-bearing massive sulfide deposits in the West
   Magnitogorsk paleoisland arc (South Urals). *Russian Geology and Geophysics*, *51*(7),
   750-763. doi:10.1016/j.rgg.2010.06.003
- Avé-Lallemand, H. G. A. (1967). Structural and petrofabric analysis of an « Alpine type »
  peridotite: The lherzolite of the French Pyrénées. *Leidse Geol. Meded.*, 42, 1-57.
- Azambre, B., & Rossy, M. (1976). Le magmatisme alcalin d'âge crétacé dans les Pyrénées
  occidentales; ses relations avec le métamorphisme et la tectonique. *Bulletin de la société Géologique de france*, 7(18), 1725-1728.
- Bailey, E. B., & McCallien, W. J. (1960). Some Aspects of the Steinmann Trinity, Mainly
  Chemical. *Quarterly Journal of the Geological Society*, *116*(1-4), 365 -395.
  doi:10.1144/gsjgs.116.1.0365
- Barbieri, M., Masi, U., & Tolomeo, L. (1979). Stable isotope evidence for a marine origin of
  ophicalcites from the north-central Apennines (Italy). *Marine Geology*, *30*(3-4), 193204. doi:10.1016/0025-3227(79)90015-X
- Barrère, P., Bouquet, C., Debroas, E.-J., Pélissonier, H., Peybernès, B., Soulé, J.-C., Souquet,
  P., et al. (1984). Carte géol. France (1/50 000), feuille Arreau (1072). Orléans.
- Barrett, T. J., & Friedrichsen, H. (1989). Stable isotopic composition of atypical ophiolitic
  rocks from east Liguria, Italy. *Chemical Geology: Isotope Geoscience section*, *80*(1),
  726 71-84. doi:10.1016/0168-9622(89)90049-3
- Bernoulli, D., & Weissert, H. (1985). Sedimentary fabrics in Alpine ophicalcites, South
   Pennine Arosa zone, Switzerland. *Geology*, *13*(11), 755-758. doi:10.1130/0091 7613(1985)13<755:SFIAOS>2.0.CO;2
- Bogoch, R. (1987). Classification and genetic models of ophicarbonate rocks. *Ofioliti*, *12*, 2336.

- Bonatti, E., Emiliani, C., Ferrera, G., Honnorez, J., & Rydell, H. (1974). Ultramafic carbonate
  breccias from the equatorial Mid-Atlantic Ridge. *Marine Geology*, *16*, 83-102.
- Bonney, T. G. (1879). Notes on some Ligurian and Tuscan serpentinites. *Geol. Mag.*, *6*(2),
  362-371.
- Bortolotti, V., & Passerini, P. (1970). Magmatic activity. *Sedimentary Geology*, 4(3-4), 599624. doi:10.1016/0037-0738(70)90024-2
- Boschi, C., Früh-Green, G., Delacour, A., Karson, J. A., & Kelley, D. S. (2006). Mass transfer
  and fluid flow during detachment faulting and development of an oceanic core
  complex, Atlantis Massif (MAR 30°N). *Geochemistry Geophysics Geosystems*, *7*, 39
  PP. doi:2006 10.1029/2005GC001074
- Boulvais P, Fourcade S, Gruau G, Moine B, Cuney M (1998) Persistance of premetamorphic
   C and O isotopic signatures in marbles subject to Pan-African granulite-facies
   metamorphism and U-Th mineralization (Tranomaro, southeast Madagascar)
   *Chemical Geology*, 150, 247-262.
- Boulvais P, de Parseval P, D'Hulst A, Paris P (2006) Carbonate alteration associated with
  talc-chlorite mineralization in the eastern Pyrenees, with emphasis on the St.
  Barthelemy Massif. Mineralogy and Petrology, 88, 499-526.
- Boulvais, P., Ruffet, G., Cornichet, J., & Mermet, M. (2007). Cretaceous albitization and
  dequartzification of Hercynian peraluminous granite in the Salvezines Massif (French
  Pyrénées). *Lithos, 93*(1-2), 89-106. doi:10.1016/j.lithos.2006.05.001
- Brotzu, P., Ferrini, V., Masi, U., Morbidelli, L., & Turi, B. (1973). Contributo alla conoscenza
  delle « Rocce Verdi » dell'Appennino centrale. Nota III. La composizione isotopica
  della calcite presente in alcuni affioramenti di oficalciti del F 129 (S. Fiora) e sue
  implicazioni petrologiche. *Period. Mineral.*, *42*, 591-619.

- Brun, J. P., & Beslier, M. O. (1996). Mantle exhumation at passive margins. *Earth and Planetary Science Letters*, *142*(1-2), 161-173. doi:10.1016/0012-821X(96)00080-5
- Burton, E. A., & Walter, L. M. (1987). Relative precipitation rates of aragonite and Mg calcite
  from seawater: Temperature or carbonate ion control? *Geology*, *15*(2), 111-114.
  doi:10.1130/0091-7613(1987)15<111:RPROAA>2.0.CO;2
- Canérot, J., & Delavaux, F. (1986). Tectonic and sedimentation on the north Iberian margin,
  Chainons Béarnais south Pyrenean zone (Pyrenees basco-béarnaises)–New data about
  the signification of the lherzolites in the Saraillé area. *Comptes Rendus de l'Académie des Sciences Series II, 302*(15), 951-956.
- Canérot, J., Peybernès, B., & Ciszak, R. (1978). Présence d'une marge méridionale à
  l'emplacement des Chaînons Béarnais (Pyrénées basco-béarnaises). *Bulletin de la société Géologique de france*, 7(20), 673-676.
- Casteras, M. (1970). Carte géol. France (1/50 000), feuille Oloron-Sainte-Marie (XV-46).
  Orléans.
- 770 Choukroune, P., et M. Séguret. 1973. « Carte structurale des Pyrénées ». ELF-ERAP.
- Choukroune, P., & ECORS Team. (1989). The Ecors Pyrenean deep seismic profile reflection
  data and the overall structure of an orogenic belt. *Tectonics*, 8(1), PP. 23-39.
  doi:198910.1029/TC008i001p00023
- Choukroune, P., & Mattauer, M. (1978). Tectonique des plaques et Pyrénées: Sur le
  fonctionnement de la faille transformante nord-Pyrénéenne; comparaisons avec les
  modèles actuels. *Bulletin de la société géologique de France, 20,* 689-700.
- Clerc, C., Lagabrielle, Y., Neumaier, M., Reynaud, J.-Y., & St Blanquat, M. (2012).
  Exhumation of subcontinental mantle rocks: evidence from ultramafic-bearing clastic
  deposits nearby the Lherz peridotite body, French Pyrenees. *Bulletin de la Societe Geologique de France*.

- 781 Clerc, C., Lagabrielle, Y., Vauchez, A., Lahfid, A., Bousquet, R., Dautria J.-M., Labaume, P.
  782 (in prep.).
- Clerc, C. 2012. « Evolution du domaine Nord-Pyrénéen au Crétacé. Amincissement crustal
  extreme et thermicité élevée: un analogue pour les marges passives ». PhD Thesis,
  Paris, France: Université Paris 6. <u>http://tel.archives-ouvertes.fr/tel-00787952</u>
- Cornelius, H. P. (1912). Petrographische untershungen in den Bergen Zwischen Septiner und Julierpass. *Diss. N. Jahr. Min.*
- Cortesogno, L., Galbiati, B., & Principi, G. (1981). Descrizione dettagliata di alcuni
  caratteristici affioramenti di brecce serpentiniche della Liguria orientale ed
  interpretazione chiave geodinamica. *Ophioliti, 6*, 47-76.
- Costa, S., & Maluski, H. (1988). Use of the 40Ar-39Ar stepwise heating method for dating
  mylonite zones: An example from the St. Barthélémy massif (Northern Pyrenees,
  France). *Chemical Geology: Isotope Geoscience section*, *72*(2), 127-144.
  doi:10.1016/0168-9622(88)90061-9
- Dauteuil, O., & Ricou, L. E. (1989). Une circulation de fluides de haute température à
  l'origine du métamorphisme crétacé nord-Pyrénéen. *Geo*, *3*(3), 237-250.
- 797 Debeaux, M., & Thiébaut, J. (1958). Les affleurements du socle paléozoique entre les massifs
  798 de la Barousse et de Milhas. *Bull. Soc. Hist. Nat. Toulouse*, *93*, 522-528.
- Debroas, E.-J. (1976). Sédimentogenèse et position structurale des flyschs crétacés du versant
  nord des Pyrénées centrales. *Bull. Bur. Rech. Géol. Min.*, *I*(4), 305-320.
- Bebroas, E.-J. (1990). Le flysch noir albo-cenomanien témoin de la structuration albienne à
  sénonienne de la Zone nord-pyrénéenne en Bigorre (Hautes-Pyrénées, France). *Bulletin de la société Géologique de france, 8*(2), 273-285.
- Bob Debroas, E.-J., Canérot, J., & Billotte, M. (2010). Les brèches d'Urdach, témoins de
  l'exhumation du manteau pyrénéen dans un escarpement de faille vraconnien-

- 806 cénomanien inférieur (zone nord-pyrénéenne, Pyrénées-Atlantiques, France). *Géologie*807 *de la France*, *2*, 53-63.
- Demange, M., Lia-Aragnouet, F., Pouliguen, M., Perrot, X., & Sauvage, H. (1999). Les
  syénites du castillet (massif de l'agly, pyrénées orientales, France): une roche
  exceptionnelle dans les pyrénées. *Comptes Rendus de l'Académie des Sciences - Series IIA Earth and Planetary Science*, *329*(5), 325-330. doi:10.1016/S12518050(00)88582-1
- Demeny, A., Vennemann, T., & Koller, F. (2007). Stable isotope compositions of the
  Penninic ophiolites of the Köszeg-Rechnitz series. *Central European Geology*, 50(1),
  29-46. doi:10.1556/CEuGeol.50.2007.1.3
- Deramond, J., Souquet, P., Fondecave-Wallez, M.-J., & Specht, M. (1993). Relationships
  between thrust tectonics and sequence stratigraphy surfaces in foredeeps: model and
  examples from the Pyrenees (Cretaceous-Eocene, France, Spain). *Geological Society, London, Special Publications, 71*(1), 193-219. doi:10.1144/GSL.SP.1993.071.01.09
- Dick, H. J. B., Tivey, M. A., & Tucholke, B. E. (2008). Plutonic foundation of a slow-
- spreading ridge segment: Oceanic core complex at Kane Megamullion, 23°30′N,
- 822 45°20'W. *Geochemistry Geophysics Geosystems*, *9*, 44 PP. doi:2008
   823 10.1029/2007GC001645 [Citation]
- Dietrich, V., Vuagnat, M., & Bertrand, J. (1974). Alpine metamorphism of mafic rocks.
   *Schweizerische Mineralogische und petrographische Mitteilungen*, *54*, 291-323.
- 826 Duée, G., Lagabrielle, Y., Coutelle, A., & Fortané, A. (1984). Les lherzolites associées aux
- 827 Chaînons Béarnais (Pyrénées Occidentales): Mise à l'affleurement anté-dogger et
  828 resédimentation albo-cénomanienne. *Comptes Rendus de l'Académie des Sciences -*829 *Serie II, 299*, 1205-1209.
- 830 Elders, Wilfred A., Robert W. Rex, Paul T. Robinson, Shawn Biehler, et Tsvi Meidav. 1972.

- « Crustal Spreading in Southern California The Imperial Valley and the Gulf of
  California Formed by the Rifting Apart of a Continental Plate ». *Science* 178 (4056)
  (juin 10): 15-24. doi:10.1126/science.178.4056.15.
- 834 Evans, C. A., & Baltuck, M. (1988). Low-Temperature Alteration of Peridotite, Hole 637A.
- 835 In G. Boillot, E. L. Winterer, & et al. (Éd.), *Proceedings of the Ocean Drilling*
- 836 *Program, 103 Scientific Results* (Vol. 103, p. 235-239). Ocean Drilling Program.
- 837 Consulté de http://www-odp.tamu.edu/publications/103\_SR/103TOC.HTM
- Fabriès, J., Lorand, J.-P., & Bodinier, J.-L. (1998). Petrogenetic evolution of orogenic
  lherzolite massifs in the central and western Pyrenees. *Tectonophysics*, *292*(1-2), 145167. doi:10.1016/S0040-1951(98)00055-9
- Fabriès, J., Lorand, J.-P., Bodinier, J.-L., & Dupuy, C. (1991). Evolution of the Upper Mantle
  beneath the Pyrenees: Evidence from Orogenic Spinel Lherzolite Massifs. *Journal of Petrology, Special\_Volume*(2), 55-76. doi:10.1093/petrology/Special\_Volume.2.55
- 844 Filleaudeau, P.-Y., F Mouthereau, et R. Pik. 2011. « Thermo-tectonic evolution of the south-
- 845 central Pyrenees from rifting to orogeny: insights from detrital zircon U/Pb and (U-
- 846 Th)He thermochronometry ». *Basin Research* 23. doi:10.1111/j.1365847 2117.2011.00535.x.
- Folk, R. L. (1974). The natural history of crystalline calcium carbonate: effects of magnesium
  content and salinity. *J. Sediment. Petrol.*, *44*, 40-53.
- Fortane, A., Duee, G., Lagabrielle, Y., & Coutelle, A. (1986). Lherzolites and the western
  « Chainons bearnais » (French Pyrenees): Structural and paleogeographical pattern. *Tectonophysics*, 129(1-4), 81-98. doi:10.1016/0040-1951(86)90247-7

- Früh-Green, G., Weissert, H., & Bernoulli, D. (1990). A multiple fluid history recorded in
  Alpine ophiolites. *Journal of the Geological Society*, *147*(6), 959-970.
  doi:10.1144/gsjgs.147.6.0959
- German, C. R., G. P. Klinkhammer, et M. D. Rudnicki. 1996. « The Rainbow Hydrothermal
  Plume, 36°15′N, MAR ». *Geophysical Research Letters* 23 (21): 2979-2982.
  doi:10.1029/96GL02883.
- Gianelli, G., & Principi, G. (1977). Northern Apennine ophiolite: an ancient transcurrent fault
  zone. *Bolletino della Societa Geologica Italiana*, *96*, 53-58.
- Gibson, I. L., Milliken, K. L., & Morgan, J. K. (1996). Serpentinite-Breccia Landslide
  Deposits Generated during Crustal Extension at the Iberia Margin. In R. B.
  Whitmarsh, D. S. Sawyer, A. Klaus, & D. G. Masson (Éd.), *Proceedings of the Ocean Drilling Program, 149 Scientific Results* (Vol. 149, p. 571-575). Ocean Drilling
  Program. Consulté de http://www-odp.tamu.edu/publications/149\_SR/149TOC.HTM
- Golberg, J.-M., & Leyreloup, A. F. (1990). High temperature-low pressure Cretaceous
  metamorphism related to crustal thinning (Eastern North Pyrenean Zone, France). *Contributions to Mineralogy and Petrology*, *104*(2), 194-207.
  doi:10.1007/BF00306443
- Golberg, J.-M., & Maluski, H. (1988). Données nouvelles et mise au point sur l'âge du
  métamorphisme pyrénéen. *C. R. Acad. Sci. Paris, 306*, 429-435.
- Golberg, J.-M., H. Maluski, et A.-F. Leyreloup. 1986. «Petrological and age relationship
  between emplacement of magmatic breccia, alkaline magmatism, and static
  metamorphism in the North Pyrenean Zone ». *Tectonophysics* 129 (1–4) (octobre 15):
  275-290. doi:10.1016/0040-1951(86)90256-8.

- Gong, Z., Langereis, C. G., & Mullender, T. A. T. (2008). The rotation of Iberia during the
  Aptian and the opening of the Bay of Biscay. *Earth and Planetary Science Letters*, *273*(1-2), 80-93. doi:16/j.epsl.2008.06.016
- Haggerty, J. A. (1987). Petrology and geochemistry of Neogene sedimentary rocks from
  Mariana forearc seamounts. In B. H. Keating, P. Fryer, R. Batiza, & G. W. Boehlert
- (Éd.), *Seamounts, Islands and Atolls* (Am. Geophys. Union, Geophys. Monogr. Ser.,
  Vol. 43, p. 175-186).
- Haggerty, J. A. (1991). Evidence from fluid seeps atop serpentine seamounts in the Mariana
  forearc: Clues for emplacement of the seamounts and their relationship to forearc
  tectonics. *Marine Geology*, *102*(1-4), 293-309. doi:10.1016/0025-3227(91)90013-T
- Henry, P., Azambre, B., Montigny, R., Rossy, M., & Stevenson, R. K. (1998). Late mantle
  evolution of the Pyrenean sub-continental lithospheric mantle in the light of new
  40Ar-39Ar and Sm-Nd ages on pyroxenites and peridotites (Pyrenees, France). *Tectonophysics, 296*(1-2), 103-123. doi:10.1016/S0040-1951(98)00139-5
- Hervouët, Y., Torné, X., Fortané, A., Duée, G., & Delfaud, J. (1987). Resédimentation
  chaotique de méta-ophites et de marbres mésozoïques de la vallée du Job (Pyrénées
- commingeoises): Relations détritisme/métamorphisme en zone nord-Pyrénéenne. *C. R. Acad. Sci.*, II, (305), 721-726.
- Jammes, S., Manatschal, G., Lavier, L. L., & Masini, E. (2009). Tectonosedimentary
  evolution related to extreme crustal thinning ahead of a propagating ocean: Example
  of the western Pyrenees. *Tectonics*, *28*(4). doi:10.1029/2008TC002406
- Kelemen, P. B., Kikawa, E., Miller, D. J., & et al. (Éd.). (2004). *Proceedings of the Ocean Drilling Program, 209 Initial Reports* (Vol. 209). Ocean Drilling Program. Consulté
  de <u>http://www-odp.tamu.edu/publications/209\_IR/209TOC.HTM</u>
- 900 Kelley, Deborah S., Jeffrey A. Karson, Donna K. Blackman, Gretchen L. Früh-Green, David

- A. Butterfield, Marvin D. Lilley, Eric J. Olson, et al. 2001. «An Off-axis
  Hydrothermal Vent Field Near the Mid-Atlantic Ridge at 30° N ». *Nature* 412 (6843)
  (juillet 12): 145-149. doi:10.1038/35084000.
- 904 Knipper, A. L. (1978). Ophicalcites and some other types of breccias accompanying the
  905 preorogenic formation of ophiolite complex. *Geotektonika*, *2*, 50-66.
- Knipper, A. L., & Sharas'kin, A. Y. (1998). Exhumation of the upper-mantle and lower-crust
  rocks during rifting. *Geotektonika*, *5*, 19-31.
- Lagabrielle, Y., & Auzende, J.-M. (1982). Active in situ disaggregation of oceanic crust and
  mantle on Gorringe Bank: analogy with ophiolitic massives. *Nature*, *297*(5866), 490493.
- Lagabrielle, Y., Bideau, D., Cannat, M., Karson, J. A., & Mével, C. (1998). Ultramafic-mafic
  plutonic rock suites exposed along the Mid-Atlantic ridge (10°N-30°N). Symmetricalasymetrical distribution and implications for seafloor spreading processes. *Faulting and magmatism at mid-ocean ridges*, Geophysical monograph (American Geophysical
  Union., p. 153-176). Washington, D.C.: Buck W. R., Delaney P. T., Karson J. A.,
  Lagabrielle Y.
- Lagabrielle, Y., & Bodinier, J.-L. (2008). Submarine reworking of exhumed subcontinental
  mantle rocks: field evidence from the Lherz peridotites, French Pyrenees. *Terra Nova*, *20*(1), 11-21. doi:10.1111/j.1365-3121.2007.00781.x
- Lagabrielle, Y., & Cannat, M. (1990). Alpine Jurassic ophiolites resemble the modern central
  Atlantic basement. *Geology*, *18*(4), 319-322. doi:10.1130/00917613(1990)018<0319:AJORTM>2.3.CO;2
- Lagabrielle, Y., Karpoff, A.-M., & Cotten, J. (1992). Mineralogical and Geochemical
  Analyses of Sedimentary Serpentinites from Conical Seamount (Hole 788A):
  Implication for the Evolution of Serpentine Seamounts. In P. Fryer, J. A. Pearce, L. B.

- Stokking, & et al. (Éd.), *Proceedings of the Ocean Drilling Program, 125 Scientific Results* (Vol. 125, p. 325-342). Ocean Drilling Program. Consulté de http://wwwodp.tamu.edu/publications/125\_SR/125TOC.HTM
- Lagabrielle, Y., Labaume, P., & St Blanquat, M. (2010). Mantle exhumation, crustal
  denudation, and gravity tectonics during Cretaceous rifting in the Pyrenean realm (SW
  Europe): Insights from the geological setting of the lherzolite bodies. *Tectonics*, 29(4).
  doi:10.1029/2009TC002588
- Lavoie, D., & Cousineau, P. A. (1995). Ordovician ophicalcites of southern Quebec
  Appalachians; a proposed early seafloor tectonosedimentary and hydrothermal origin. *Journal of Sedimentary Research*, 65(2a), 337-347. doi:10.1306/D42680B8-2B26-
- 936 11D7-8648000102C1865D
- 937 Laznicka, P. (1988). Breccias and Coarse Fragmentites: Petrology, Environments,
  938 Associations, Ores. Elsevier Science Ltd.
- 939 Le Pichon, X., Bonnin, J., & Sibuet, J.-C. (1970). La faille nord-Pyrénéenne: Faille
  940 transformante liée à l'ouverture du Golfe de Gascogne. *Comptes Rendus de*941 *l'Académie des Sciences*, D, *271*, 1941-1944.
- Lemoine, M. (1980). Serpentinites, gabbros and ophicalcites in the Piemont-Ligurian domain
  of the Western Alps: Possible indicators of océanic fracture zone and of associated
  serpentinite protrusions in the Jurassic-Cretaceous Thetys. *Archives des Sciences Genèves, 33*, 103-115.
- Lemoine, M., Tricart, P., & Boillot, G. (1987). Ultramafic and gabbroic ocean floor of the
  Ligurian Tethys (Alps, Corsica, Apennines): In search of a genetic imodel. *Geology*, *15*(7), 622-625. doi:10.1130/0091-7613(1987)15<622:UAGOFO>2.0.CO;2
- 949 Lucazeau, Francis, Sylvie Leroy, Frédérique Rolandone, Elia d' Acremont, Louise Watremez,
  950 Alain Bonneville, Bruno Goutorbe, et Doga Düsünur. 2010. «Heat-flow and

- hydrothermal circulation at the ocean–continent transition of the eastern gulf of
  Aden ». *Earth and Planetary Science Letters* 295 (3–4) (juillet 1): 554-570.
  doi:10.1016/j.epsl.2010.04.039.
- Manatschal, G. (2004). New models for evolution of magma-poor rifted margins based on a
  review of data and concepts from West Iberia and the Alps. *International Journal of Earth Sciences*, *93*(3), 432-466. doi:10.1007/s00531-004-0394-7
- Mattauer, M., & Choukroune, P. (1974). Les lherzolites des Pyrénées sont des extrusions de
  matériel ancien dans le Mésozoique nord Pyrénées. *paper presented at 2nd Réunion Annuelle des Sciences de la Terre, Soc. Géol. de Fr., Paris.*
- McCrea, J. M. (1950). On the isotope chemistry of carbonates and a paleotemperature scale. *J. Chem. Phys.*, *18*, 849-857.
- Milliken, K. L., & Morgan, J. K. (1996). Chemical Evidence for Near-Seafloor Precipitation
  of Cacite in Serpentinites (Site 897) and Serpentinite Breccias (Site 899), Iberia
  Abyssal Plain. In R. B. Whitmarsh, D. S. Sawyer, A. Klaus, & D. G. Masson (Éd.),
- 965 *Proceedings of the Ocean Drilling Program, 149 Scientific Results* (Vol. 149, p. 553-
- 966 558). Ocean Drilling Program. Consulté de http://www967 odp.tamu.edu/publications/149\_SR/149TOC.HTM
- Minnigh, L. D., van Calsteren, P. W. C., & den Tex, E. (1980). Quenching: An additional
  model for emplacement of the Iherzolite at Lers (French Pyrenees). *Geology*, 8(1), 18.
  doi:10.1130/0091-7613(1980)8<18:QAAMFE>2.0.CO;2
- Moine, B., Fortune, J. P., Moreau, P., & Viguier, F. (1989). Comparative mineralogy,
  geochemistry, and conditions of formation of two metasomatic talc and chlorite
  deposits; Trimouns (Pyrenees, France) and Rabenwald (Eastern Alps, Austria). *Economic Geology*, *84*(5), 1398 -1416. doi:10.2113/gsecongeo.84.5.1398

- 975 Monchoux, P. (1970). Les lherzolites pyrénéennes: contribution à l'étude de leur minéralogie,
  976 de leur génèse et de leurs transformations (Thèse d'Etat). Univ. Toulouse.
- Montigny, R., Azambre, B., Rossy, M., & Thuizat, R. (1986). K-Ar Study of cretaceous
  magmatism and metamorphism in the pyrenees: Age and length of rotation of the
  liberian Peninsula. *Tectonophysics*, *129*(1-4), 257-273. doi:10.1016/00401951(86)90255-6
- Morgan, J. K., & Milliken, K. L. (1996). Petrography of Calcite Veins in Serpentinized
  Peridotite Basement Rocks from the Iberia Abyssal Plain, Sites 897 and 899:
  Kinematic and Environmental Implications. In R. B. Whitmarsh, D. S. Sawyer, A.
  Klaus, & D. G. Masson (Éd.), *Proceedings of the Ocean Drilling Program, 149*
- 985 Scientific Results (Vol. 149, p. 559-569). Ocean Drilling Program. Consulté de
   986 <u>http://www-odp.tamu.edu/publications/149\_SR/149TOC.HTM</u>
- Muffler, L. J. Patrick, et Donald E. White. 1969. « Active Metamorphism of Upper Cenozoic
  Sediments in the Salton Sea Geothermal Field and the Salton Trough, Southeastern
- 989 California ». *Geological Society of America Bulletin* 80 (2) (janvier 2): 157-182.
- 990 doi:10.1130/0016-7606(1969)80[157:AMOUCS]2.0.CO;2.
- Muñoz, J. A. (1992). Evolution of a continental collision belt: ECORS-Pyrenees crustal
  balanced cross-section. *Thrust Tectonics* (Chapman and Hall., p. 235-246). London:
  K. McClay.
- Ohnenstetter, M. (1979). La série ophiolitifère de Rospigliano (Corse) est-elle un témoin des
  phénomènes tectoniques, sédimentaires et magmatiques liés au fonctionnement des
  zones transformantes? *Comptes Rendus de l'Académie des Sciences, Paris*, D, *289*,
  1199-1202.
- 998 Olivet, J. L. (1996). La cinématique de la plaque ibérique. *Bull. Cent. Rech. Explor. Prod. Elf-*999 *Aquitaine*, 20(1), 131-195.

Passchier, C. W. (1984). Mylonite-Dominated Footwall Geometry in a Shear Zone, Central
Pyrenees. *Geological Magazine*, *121*(05), 429-436. doi:10.1017/S0016756800029964

- Peters, T. (1965). A water-bearing andradite from the Totalp serpentine (Davos, Switzerland). *Am*, *50*, 1482-1486.
- Picazo, S., Cannat, M., Delacour, A., Escartin, J., Rouméjon, S., & Silantyev, S. (2012).
  Deformation associated with the denudation of mantle-derived rocks at the MidAtlantic Ridge 13°-15°N: the role of magmatic injections and hydrothermal alteration. *Geochemistry Geophysics Geosystems*. doi:10.1029/2012GC004121
- Plas, A. (1997). Petrologic and stable isotope constraints on fluid-rock interaction,
   serpentinization and alteration of oceanic ultramafic rocks (PhD Thesis). Swiss
   Federal Institute of Technology., Swiss.
- Poujol, M., Boulvais, P., & Kosler, J. (2010). Regional-scale Cretaceous albitization in the
   Pyrenees: evidence from in situ U-Th-Pb dating of monazite, titanite and zircon.
   *Journal of the Geological Society*, *167*(4), 751-767. doi:10.1144/0016-76492009-144
- 1014 Puigdefàbregas, C., & Souquet, P. (1986). Tecto-sedimentary cycles and depositional
- sequences of the Mesozoic and Tertiary from the Pyrenees. *Tectonophysics*, *129*(1-4),

1016 173-203. doi:10.1016/0040-1951(86)90251-9

- 1017 Ravier, J. 1959. « Le métamorphisme des terrains secondaires des Pyrénées ». *Mem. Soc.*
- 1018 *Geol. Fr.* 86: 1-250.
- 1019 Ross, D. J. (1991). Botryoidal high magnesium calcite cements from the upperCretaceous of
  1020 the Mediterranean region. *J*, *61*, 349-353.
- Roure, F., & Combes, P.-J. (1998). Contribution of the ECORS seismic data to the Pyrenean
  geology: Crustal architecture and geodynamic evolution of the Pyrenees. Consulté
  de http://cat.inist.fr/?aModele=afficheN&cpsidt=1874322

- Schärer, U., de Parseval, P., Polvé, M., & St Blanquat, M. (1999). Formation of the Trimouns
  talc-chlorite deposit (Pyrenees) from persistent hydrothermal activity between 112 and
  97 Ma. *Terra Nova*, *11*(1), 30-37. doi:10.1046/j.1365-3121.1999.00224.x
- Schwarzenbach, E. (2011). Serpentinization, fluids and life: comparing carbon and sulfur
   *cycles in modern and ancient environments* (PhD Thesis). Swiss Federal Institute of
   Technology., Zurich.
- 1030 Skelton, A. D. ., & Valley, J. W. (2000). The relative timing of serpentinisation and mantle
  1031 exhumation at the ocean-continent transition, Iberia: constraints from oxygen isotopes.
  1032 *Earth and Planetary Science Letters*, *178*(3-4), 327-338. doi:10.1016/S00121033 821X(00)00087-X
- Smart, P. L., Palmer, R. J., Whitaker, F., & Wright, V. P. (1987). Neptunian dikes and
  fissures fills: an overview and account of some modern exemples. In N. P. James & P.
  W. Choquette (Éd.), *Paleokarst* (Springer-Verlag., p. 149-163). New York.
- Souquet, P., Debroas, E.-J., Boirie, J.-M., Pons, P., Fixari, G., Dol, J., Thieuloy, J.-P., et al.
  (1985). Le groupe du Flysch noir (albo-cénomanien) dans les Pyrénées. *Bull. centres*

1039 *de Rech. Exlpo.-Prod. Elf-Aquitaine, Pau, 9*(1), 183-252.

- Spooner, E. T. C., & Fyfe, W. S. (1973). Sub-sea-floor metamorphism, heat and mass
  transfer. *Contributions to Mineralogy and Petrology*, *42*(4), 287-304.
  doi:10.1007/BF00372607
- St Blanquat, M. (1993). La faille normale ductile du massif du Saint Barthélémy: Evolution
  hercynienne des massifs nord-pyrénéens catazonaux considérée du point de vue de
  leur histoire thermique. *Geodin. Acta, 6*(1), 59-77.
- St Blanquat, M., Brunel, M., & Mattauer, M. (1986). Les zones de cisaillements du massif
  nord Pyrénéen du Saint-Bartelemy, témoins probables del'extension crustale d'âge
  crétacé. *C*, *303*, 1339-1344.

- St Blanquat, M., Lardeaux, J. M., & Brunel, M. (1990). Petrological arguments for hightemperature extensional deformation in the Pyrenean Variscan crust (Saint Barthélémy
  Massif, Ariège, France). *Tectonophysics*, *177*(1-3), 245-262. doi:10.1016/00401951(90)90284-F
- Surour, A. A., & Arafa, E. H. (1997). Ophicarbonates: calichified serpentinites from Gebel
   Mohagara, Wadi Ghadir area, Eastern Desert, Egypt. *Journal of African Earth Sciences*, 24(3), 315-324. doi:10.1016/S0899-5362(97)00046-8
- Teixell, A. (1998). Crustal structure and orogenic material budget in the west central
  Pyrenees. *Tectonics*, 17(3), 395-406. doi:199810.1029/98TC00561
- 1058 Ternet, Yves, M. Colchen, Elie-Jean Debroas, B. Azambre, F. Debon, J.-L. Bouchez, G.
  1059 Gleizes, et al. 1997. *Notice explicative, Carte géol. France (1/50 000), feuille Aulus*
- 1060 *les Bains (1086).* BRGM éd. Orléans: BRGM.
- Thiébaut, J., Debeaux, M., Durand-Wackenheim, C., Souquet, P., Gourinard, Y., Bandet, Y.,
  & Fondecave-Wallez, M.-J. (1988). Métamorphisme et halocinèse crétacés dans les
  évaporites de Betchat le long du chevauchement frontal Nord-Pyrénéen (HauteGaronne et Ariège, France). *C. R. Acad. Sci. Paris*, *307*(13), 1535-1540.
- 1065 Thiébaut, J., Durand-Wackenheim, C., Debeaux, M., & Souquet, P. (1992). Métamorphisme
  1066 des évaporites triasiques du versant nord des Pyrénées centrales et Occidentales. *Bull.*1067 *Soc. Hist. Nat. Toulouse*, *128*, 77-84.
- Treves, B. E., & Harper, G. D. (1994). Exposure of serpentinites on ocean floor. Sequence of
  faulting and hydrofracturing in the Northern Apennine ophicalcites. *Ophioliti*, *19*, 435466.
- 1071 Treves, B. E., Hickmott, D., & Vaggelli, G. (1995). Texture and microchemical data of
  1072 oceanic hydrothermal calcite veins, Northern Apennine ophicalcites. *Ophioliti*, 20(2),
  1073 111-122.

- 1074 Trommsdorff, V., Evan, B. W., & Pfeifer, H. R. (1980). Ophicarbonate rocks: metamorphic
  1075 reactions and possible origin. *Archives des Sciences Genève*, *33*, 361-364.
- 1076 Valley, J.W., 1986. Stable isotope geochemistry of metamorphic rocks. In: Valley, J.W.,
  1077 Taylor, H.P., Jr., O'Neil, J.R. Eds.., Stable Isotopes in High Temperature Geological
  1078 Processes. *Reviews in Mineralogy*, Vol. 16. Mineral. Soc. Am., 445–489.
- 1079 Vergés, J., & Garcia-Senz, J. (2001). Mesozoic evolution and Cainozoic inversion of the
- 1080 Pyrenean rift. Peri-Tethys Memoir 6: Peri-Tethyan Rift/Wrench Basins and Passive
- Margins (Mem. Mus. Natl. Hist. Nat., p. 187-212). Paris: P. A. Ziegler et al. Consulté
   de http://www.ija.csic.es/gt/gdl/jverges/PDF/Verges\_Garcia\_2001.pdf
- 1083 Vielzeuf, D. (1984). *Relations de phases dans le faciès granulite et implications* 1084 géodynamiques. L'exemple des granulites des pyrénées. (Thèse). Clermont-Ferrand.
- 1085 Vielzeuf, D., & Kornprobst, J. (1984). Crustal splitting and the emplacement of Pyrenean
  1086 lherzolites and granulites. *Earth and Planetary Science Letters*, *67*(1), 87-96.
  1087 doi:10.1016/0012-821X(84)90041-4
- 1088 Vissers, R. L. M., Drury M. R., Newman J., & Fliervoet T. F. (1997). «Mylonitic
  1089 deformation in upper mantle peridotites of the North Pyrenean Zone (France):
  1090 implications for strength and strain localization in the lithosphere ». *Tectonophysics,*1091 279, 303-325. doi:10.1016/S0040-1951(97)00128-5.
- Weissert, H., & Bernoulli, D. (1984). Oxygen isotope composition of calcite in Alpine
  ophicarbonates: a hydrothermal or Alpine metamorphic signal ? *Eclogae geol. Helv.*,
  77(1), 29-43.
- Wicks, F. J., & Whittaker, E. J. W. (1977). Serpentine textures and serpentinization. *The Canadian Mineralogist*, *15*(4), 459 -488.

- Winterer, E. L., Metzler, C. V., & Sart, M. (1991). Neptunian dykes and associated breccias
  (Southern Alps, Italy and Switzerland): role of gravity sliding in open and closed
  systems. *Sedimentology*, *38*(3), 381-404. doi:10.1111/j.1365-3091.1991.tb00358.x
- 1100 Zheng, Y. F. (2011). On the theoretical calculations of oxygen isotope fractionation factors
- 1101 for carbonate-water systems. *Geochemical Journal*, *45*, 341-354.

## 1103 Table Caption

1104

- 1105 **Table 1:** C (vs. PDB) an O (vs. SMOW) isotopes compositions determined for the carbonate
- 1106 fraction of the veins, matrix and clasts from the Pyrenean ophicalcite.
- **Table 2:** Schematic representation of the different types of ophicalcites analyzed in this study.

1109 Figure Caption

1110

1111 Figure 1. Simplified geological map of the Northern Pyrenean belt with location of the1112 peridotite bodies sampled in this study.

1113

Figure 2. A: Simplified geological map of the Urdach and Tos de la Coustette in the Mail Arrouy and Sarrance *Chaînons Béarnais* with sample sites. B: Simplified geologic map of the Aulus basin presenting the extent of exposure of the peridotite bearing deposits surrounding the *Etang de Lherz* area with the location of the Freychinède, Fontête Rouge, and Berqué samples sites.

1119

Figure 3: Photograph of an ultramafic olistolith in the Aulus basin illustrating the progressivetransition from polymictic breccias to massive peridotite penetrated by calcitic veins

1122

Figure 4: Macroscopic aspects of some of the western Pyrenean ophicalcites. A and B: development of calcites veins along tectonic discontinuities in the Urdach peridotite body. C: Mesh texture in highly serpentinized peridotite of Tos de la Coustette. D: Pervasive carbonation and veins in Tos de la Coustette peridotite. Calcite veins (E) and cavities infillings (F) in the Moncaup ultramafic body.

1128

Figure 5: Macroscopic aspects of some of the eastern Pyrenean ophicalcites. A: Bimodallitharenite presenting slumps and syn-sedimentary normal faults from Lherz. B: Grain sorting

in polymictic litharenites from Lherz. C and D: Breccia reworking fresh (orange to green) and
serpentinized (dark green to black) peridotites in a calcitic matrix from the Lherz ophicalcites.
E: Close association of matrix and veins in a typical ophicalcite from Vicdessos. F: Exposure
of an ultramafic body presenting a centimetric orange-brown oxidation ring on the contact
between peridotites and carbonates (Ercé-Angladure) G: Metric-sized mesh texture in the
Bestiac peridotites. H: Detail of F showing calcite veins cross-cutting the latest serpentinite
veins.

1138

Figure 6: Microscopic aspects of the Pyrenean ophicalcites. A: Seal crack calcite vein from Urdach in cathodoluminescence (CL) and redrawn. B: Micrometric veinlets from Urdach. C: Botryoidal calcite in a vein from Urdach, in transmitted light and CL. D: Replacement texture of the ophicalcites from Tos de la Coustette, polarized light. F: Clear sparry calcite in veins from Lherz. G: Close vein/matrix association in transmitted light and CL. H: Dogtooth calcite ghosts in recrystallized veins, in polarized light and Redrawn.

1145

Figure 7: δ<sup>13</sup>C vs. d18O diagram showing the isotopic compositions of the Pyrenean
ophicaclites (veins, matrices and clasts). Shaded areas represent values from the literature for
ophicalcites from the Iberian margin and Galicia bank (Evans & Baltuck 1988; Milliken &
Morgan 1996; Plas 1997; Skelton & Valley 2000); the Alps and Apennines (Brotzu et al.
1973; Barbieri et al. 1979; Weissert & Bernoulli 1984; Barrett & Friedrichsen 1989; Demeny
et al. 2007) and from other hydrothermal ophicalcites (Lavoie & Cousineau 1995; Artemyev
& Zaykov 2010).

Figure 8: Comparison of the C and O isotope compositions of calcitic veins and matrices inthe ophicalcites from Eastern Pyrenees.

1156

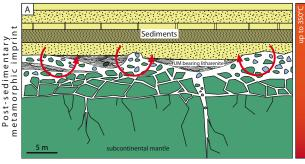
Figure 9: Comparison of calcite microtextures in veins and matrices from this study and fromthe Iberian margin (Morgan & Milliken, 1996).

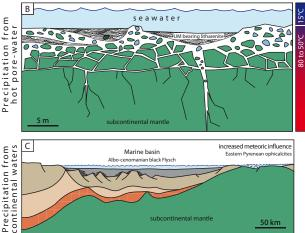
1159

Figure 10: Cartoons illustrating the three possible mechanisms responsible the low Ocomposition of the sedimentary ophicalcites from the Eastern Pyrenees.

1162

Figure 11: Sketches presenting the exhumation history of the Eastern and Western Pyrenean peridotites in the light of our isotope study. Serpentinization processes are represented by green colors and the formation of ophicalcites by blue colors.



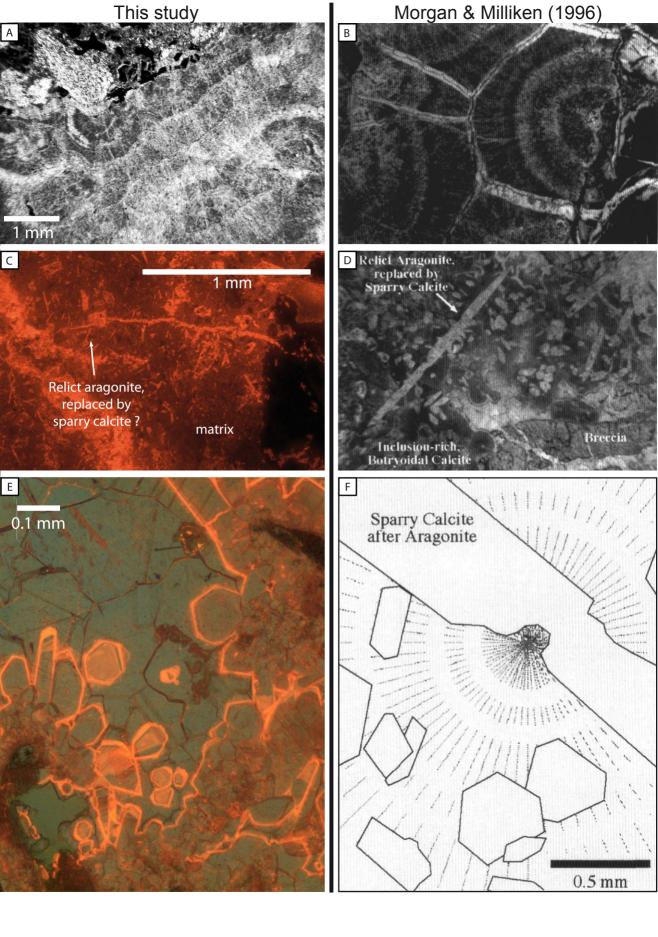


HT-LP Cretaceous Metamorphism

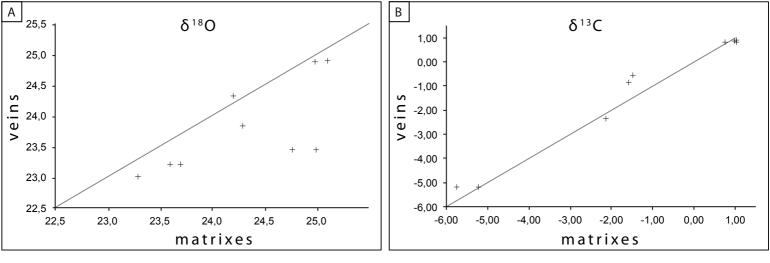
gradient

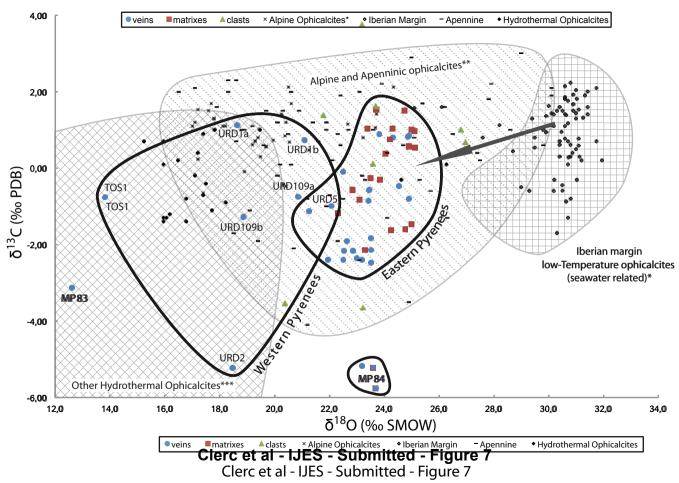
thermal

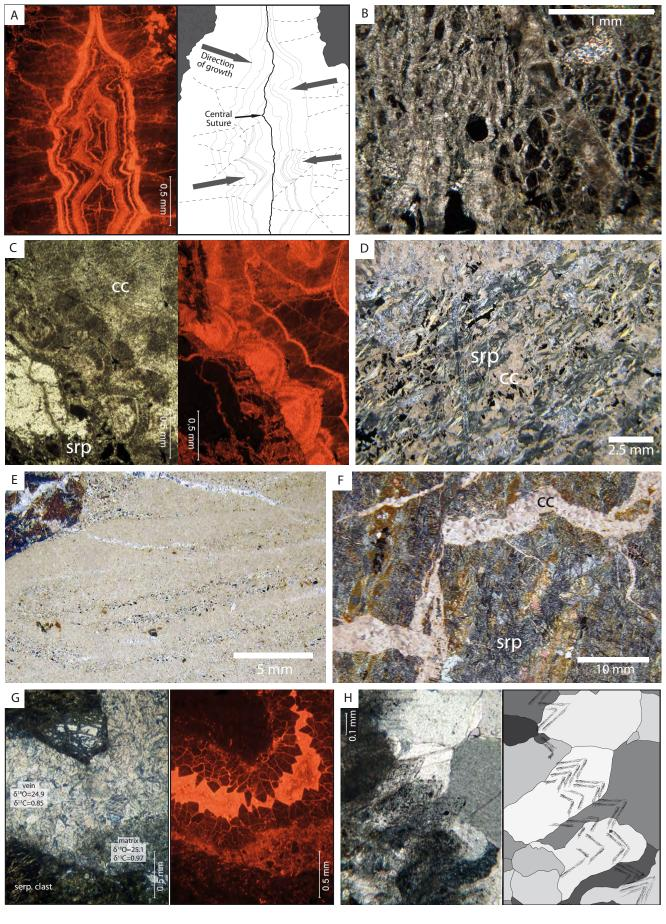
steep



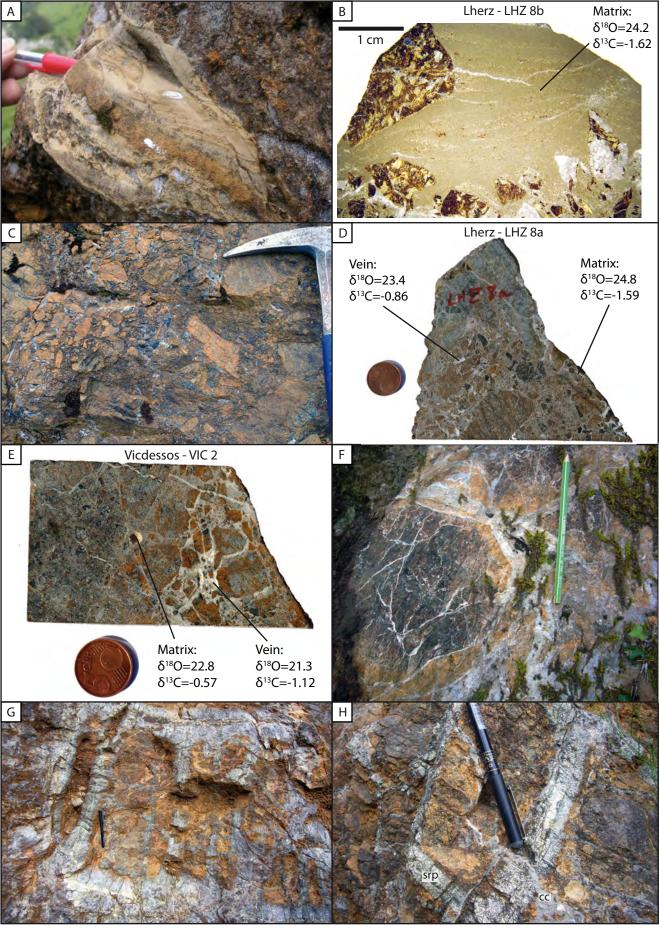
Clerc et al - IJES - Submitted - Figure 9



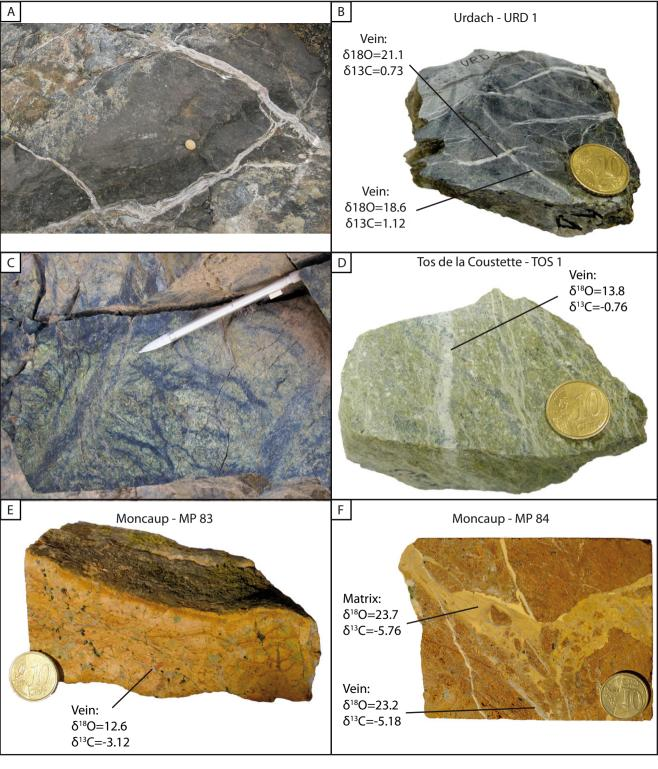




Clerc et al - IJES - Submitted - Figure 6

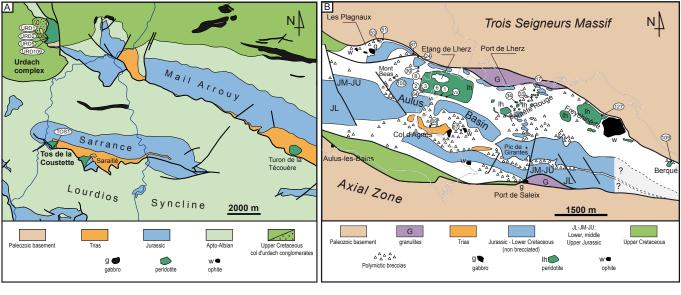


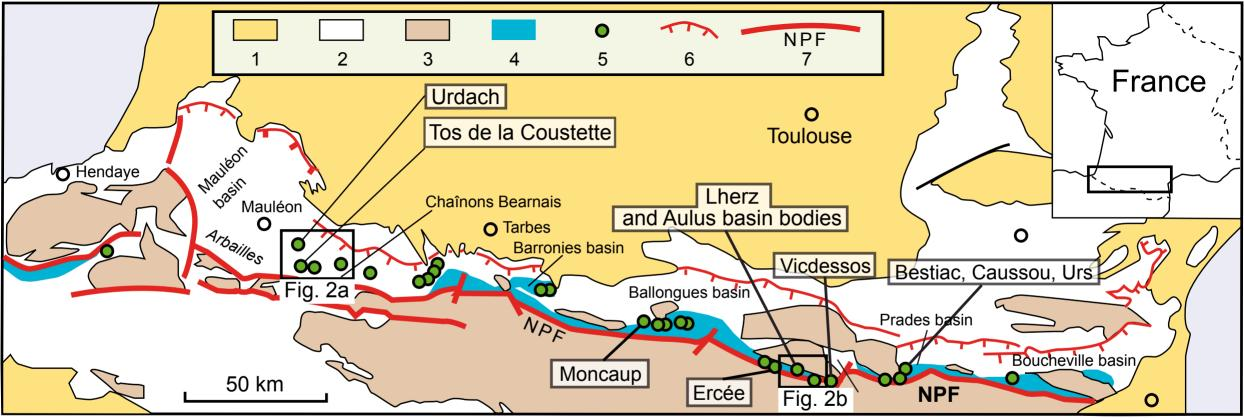
Clerc et al - IJES - Submitted - Figure 5



Clerc et al - IJES - Submitted - Figure 4







1,Oligocène and post-Oligocène; 2, Mesozoic and Eocene; 3, Paleozoic Basement; 4, area of HT-LP Pyrenean metamorphism; 5, peridotite; 6, main external thrusts; 7, North Pyrenean Fault (NPF)

